CHALMERS

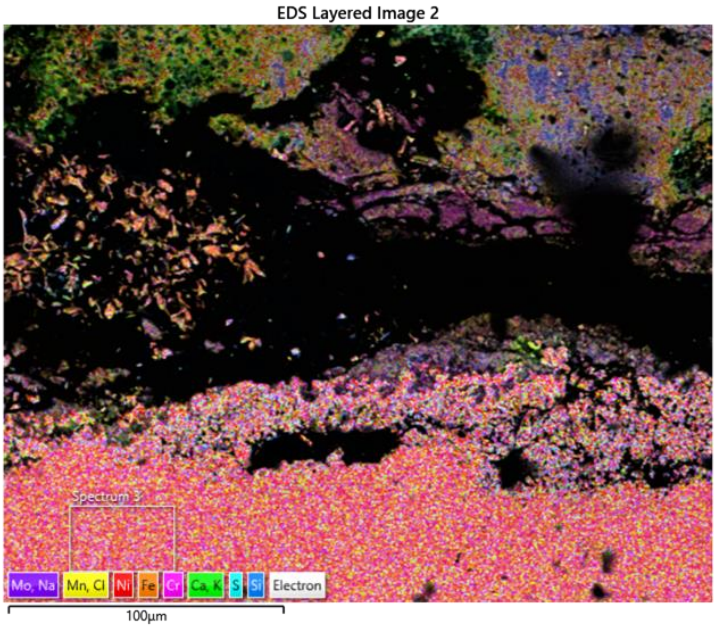

The effect of fuel on the corrosion rate of commercial steels- a field study

Bachelor thesis in chemical engineering

Robin Berndt
Samuel Nilsson Becerra

DEPARTMENT OF CHEMISTRY AND CHEMICAL ENGINEERING
CHALMERS UNIVERSITY OF TECHNOLOGY
Gothenburg, Sweden 2023
www.chalmers.se

The effect of fuel on the corrosion rate of commercial steels - a field study

Robin Berndt and Samuel Nilsson Becerra

Supervisor: Maria Dolores Paz Olausson, Senior Research engineer, Department of chemistry and chemical engineering
Examiner: Jesper Liske, Docent, Department of chemistry and chemical engineering

Technical report
Department of chemistry and chemical engineering
Chalmers University of Technology
SE-412 96 Göteborg
Sweden
Telephone +46 031-772 1000

Acknowledgements

We would like to thank our supervisor Loli for her unwavering aid and guidance throughout the project. We also want to thank our examiner Jesper for giving us the opportunity to do this study.

The effect of fuel on the corrosion rate of commercial steels – A field study

Robin Berndt, Samuel Nilsson Becerra
Department of Chemistry and Chemical Engineering
Chalmers University of Technology

Abstract

This study focuses on investigating the effects of long-term exposure of different steel alloy samples in the superheater region of two boilers, situated in Biganos (Biomass fuel) and Grenoble (waste fuel). The purpose of this study is to analyze the corrosion mechanisms of various commercially used stainless-steel alloys and compare their costs to fulfill the goal of determining the most suitable alloy in terms of lifetime and maintenance cost. The value of this research is based upon the increasing global need for fuels in power and heat production as well as the need to solve both environmental and economic challenges associated with fossil fuels. It is of great value that the construction of future powerplants and especially boilers is constructed of high temperature corrosion resistant materials, both regarding the economical perspective of the companies but also concerning the global goals of environmental sustainability. The samples were analyzed using Scanning Electron Microscopy (SEM) together with Energy Dispersive X-ray Spectroscopy (EDX) in order to calculate material loss, due to corrosion, and chemical composition of attached deposit layers. Additionally, Ion Chromatography (IC) was used to investigate the presence of chlorine and sulfur containing compounds. This study presents data which indicates a great variation in corrosion resistance between steel alloys. Some samples showed signs of great material loss together with a dense and solid deposit layer and other samples showed little to no material loss. In conclusion the material with the most suitable properties for the two boilers is AISI TP310H with no significant material loss and a relatively low price.

List of Contents

1. Introduction 2
1.1 Background 2
1.2 Effects of using renewable fuels 2
1.3 Oxide layers 2
1.4 Research task 3
1.5 Goal 3
2. Description of the boilers 4
2.1 Biomass boiler 4
2.2 Waste boiler 5
3. Materials 6
3.1 P91 6
3.2 Sanicro 28 7
3.3 13CrMo4-5 7
3.4 AISI TP310H 7
4. Research method 7
4.1 Preparing sample 7
4.2 Scanning Electron Microscope/Energy-dispersive X-Ray spectroscopy 8
4.3 Ion Chromatography 8
5. Result and Discussion 9
5.1 Scanning Electron Microscope images and EDX data 9
5.1.1 Biomass 500 °C Samples 10
5.1.2 Waste 500 °C Samples 16
5.1.3 Biomass 600 °C samples 25
5.1.4 Waste 600 °C Samples 27
5.1.5 EDX data for 600 °C samples 28
5.2 Material Loss of samples 28
5.2.1 Biomass boiler samples at 500 °C 28
5.2.2 Waste boiler samples 500 °C 29
5.2.3 Biomass boiler samples 600 °C 31
5.2.4 Waste boiler samples 600 °C 31
5.3 Ion Chromatography 31
5.3.1 Biomass boiler samples 32
5.3.2 Waste boiler samples 33
6. Conclusions 34
7. Goal fulfilment and future research 34
8. Literature references 35

9. Appendices..36

List of Figures

Figure 1. Picture of the probe where the samples were attached 4
Figure 2. Schematic of the Biomass boiler in Biganos 5
Figure 3. Schematic of the Waste boiler in Grenoble 6
Figure 4. SEM image of P91 sample from Biomass boiler at 500 °C 10
Figure 5. EDX map of P91 at 500 °C in the biomass boiler 11
Figure 6. SEM image of Sanicro 28 sample from Biomass boiler at 500 °C 12
Figure 7. EDX map 1 of Sanicro 28 from Biomass boiler at 500 °C 13
Figure 8. EDX map 2 of Sanicro 28 from Biomass boiler at 500 °C 14
Figure 9. SEM image of AISI TP310H sample from Biomass boiler at 500 °C 14
Figure 10. EDX map of AISI TP310H from Biomass boiler at 500 °C 15
Figure 11. SEM image of P91 sample from Waste boiler at 500 °C 17
Figure 12. EDX map 1 of P91 from Waste boiler at 500 °C 18
Figure 13. EDX map 2 of P91 from Waste boiler at 500 °C 19
Figure 14. SEM image of 13CrMo4-5 sample from Waste boiler at 500 °C 20
Figure 15. EDX map 1 of 13CrMo4-5 from Waste boiler at 500 °C 21
Figure 16. EDX map 2 of 13CrMo4-5 from Waste boiler at 500 °C 22
Figure 17. SEM image of AISI TP310H from Waste boiler at 500 °C 23
Figure 18. EDX map 1 of AISI TP310H from Waste boiler at 500 °C 24
Figure 19. EDX map 2 of AISI TP310H from Waste boiler at 500 °C 25
Figure 20. SEM image of P91 from Biomass boiler at 600 °C 26
Figure 21. SEM image of Sanicro 28 from Biomass boiler at 600 °C 26
Figure 22. SEM image of AISI TP310H from Biomass boiler at 600 °C 27
Figure 23. SEM image of Sanicro 28 from Waste boiler at 600 °C 27
Figure 24. SEM image of AISI TP310H from Waste boiler at 600 °C 28
Figure 25. Material loss of P91 in Biomass boiler at 500 °C after 3000h 28
Figure 26. Material loss of Sanicro 28 in Biomass boiler at 500 °C after 3000h 29
Figure 27, Material loss of AISI TP310H in Biomass boiler at 500 °C after 3000h 29
Figure 28. Material loss of P91 in Waste boiler after 1000h 30
Figure 29. Material loss of 13CrMo4-5 in Waste boiler at 500°C after 1000h 30
Figure 30. Material loss of AISI TP310H in Waste boiler at 500 °C after 1000h 30
Figure 31. Difference in amount of SO4 in deposit of Biomass samples at 500 °C and 600 °C 32
Figure 32. Difference in amount of Cl in deposit of Biomass samples at 500 °C and 600 °C 33
Figure 33. Difference in amount of SO4 in deposit of Waste samples at 500°C and 600°C 33
Figure 34. Difference in amount of Cl in deposit of Waste samples at 500°C and 600°C 34

List of tables

Table 1. Samples in the boilers 4
Table 2. Percentage of elements in each metal sample 6
Table 3. Standard samples of SO4 and Cl 9
Table 4. Amount of each element in a specific part of the sample (See figure. 10) 16
Table 5. Amount of each element in a specific part of the sample (See figure. 10) 16
Table 6. Amount of each element in a specific part of the sample (See figure. 13) 19
Table 7. Amount of each element in a specific part of the sample (See figure 13.) 20
Table 8. Average and maximum material loss of 500°C biomass samples 29
Table 9. Average and maximum material loss of 500 °C waste samples 31
Table 10. Average and maximum material loss of 600 °C biomass samples 31
Table 11. Average and maximum material loss of 600 °C waste samples 31
Table 12. Biomass samples IC result 32
Table 13. Waste samples IC result 33

List of abbreviations

SEM	Spectrum Electron Microscopy
EDX	Energy Dispersive X-ray spectroscopy
IC	Ion Chromatography

1. Introduction

1.1 Background

To fulfill the globally increasing need for fuels in heat and power production while simultaneously not aiding in increasing the environmental effect in the world has become a problem that more and more companies want a solution to. The increasing need of power and heat comes from the growing population and electrification across the world, and it will continue to increase as long as the population does. At present times the majority of power and heat around the world comes from fossil fuel powerplants as these plants are cheaper and more effective than the options using renewable fuels that exist on market today [1-2]. In order for the renewable fuel power plants to win the economic competition that they are currently losing the cost of operating the power plants must be lowered or the capacity of power production must increase. This can be done in a multitude of ways such as increasing the output of power from the power plant or reducing the costs of operating the power plant. Increasing the output of the power plant can be done by increasing the steam temperature but the increased operating temperature will require more corrosion resistant materials. Reducing the cost of operating the power plant can also be done by using cheaper fuels, which in many cases contain more corrosive species. Finally reducing the maintenance costs of the plant can also lead to a reduction of the total production cost. All three of these challenges can be solved by constructing the superheaters in the power plants out of corrosive resistant materials such as steel alloyed with chromium and nickel. Optimization of the material selection regarding the corrosion level inside the boiler are critical when constructing and play a big role in lowering the environmental effect of the power plant. [3]

1.2 Effects of using renewable fuels

The drawback from using more renewable fuels such as waste or biomass results in a fuel gas with low concentrations of sulfate ions (SO_4^-) and high concentrations of alkali- and hydrogen chlorides (HCl) [3]. These alkali species can then react with the chromium in the oxide of the metal and deprive it from its protective layer, while forming alkali chromates. This results in a fast-growing iron oxide that give poor protection to the metal. With decreased protection the speed of corrosion increases and may cause damage to the superheaters which leads to unwanted shutdowns of the operation.

One way to avoid the increased corrosion rate is to lower the operating temperature of the boiler, lowering the temperature will result in less production and with-it decreased revenue. Another way to avoid the increased corrosion is to convert the alkali chlorides to alkali sulphates. Adding compounds containing sulphur to the fuel of boiler have been reported to decrees the rate of corrosion by 50% - 70%. However, there is no way of knowing how adding sulphur to the fuel will affect future corrosion rates of the boiler [5].

1.3 Oxide layers

A metal alloy cannot resist high temperature corrosion by itself. For the alloy to be able to handle high temperature corrosion it needs to form a protective oxide layer, the so called passive film, which acts as a barrier between the metal and the corrosive substances, of either iron oxide or an oxide of its alloys. The amount of protection and the corrosive properties of the alloys depend on different factors, such as the growth rate, chemical reactivity, adhesion,

and the mechanical properties of the alloy. The most common protective oxide layers in waste and biomass burners are iron oxides, chromium oxides and nickel oxides. Out of these three oxides the nickel oxides are the most protective, followed by chromium and at last iron. When nickel oxidizes it forms a NiO oxide layer. Chromium oxidizes and forms Cr_2O_3 and iron forms Fe_2O_3. All three creates a layer around the metal that protects it from further oxidation and corrosion [4].

The difference between iron, chromium and nickel oxides is that iron oxide forms at a faster pace than chromium and nickel oxide, which results in a poorer corrosion protection and a much more porous oxide layer which breaks away easier leaving the metal exposed. Exposed metal will then corrode away or continue to form porous iron oxide. Therefore, the rate of oxide layer build up is one key factor to the alloys ability to withstand corrosion. However, it is not only the speed of oxidation that is important. When for example a chromium steel alloy oxidizes it quickly forms an oxide layer that protects the alloy from further oxidation but then the growth slows down and the layer remains thin. The key is to find a composition that forms a thin but dense and non-porous oxide layer. Another advantageous property is the alloys' ability to "self-repair" by diffusion of for example chromium to the scale surface when damaged. In some alloys other trace elements such as silicone help enhance the protective properties by in the case of silicone forming a thin layer of silicone oxide (SiO_2) underneath the chromium oxide scale [6].

1.4 Research task

The main aim of this report is to study the environment in the superheater region of two different boilers (one biomass fired and one waste fired) and to analyse the corrosion mechanisms of different commercially used steels when exposed to the superheater region of each boiler as well as compare costs of different materials to provide the best suitable alloy regarding both lifespan and cost.

The main focus of investigation in this study was:

- Long term exposure to corrosive environment of different samples in different boilers
- Material loss of different samples
- Corrosion at different temperatures
- Composition of coating deposit of exposed samples

This study made use of different methods to investigate the named tasks, it made use of a scanning electron microscope (SEM), energy dispersive x-ray spectroscopy (EDX) and ion chromatography (IC).

1.5 Goal

The overall goal of the study is to gather data about different metals that can be used to construct the superheater region of the boiler and thereby improve the overall economy of the boiler and electricity production. The materials studied in this project are part of the BELENUS EU financed project and consist of commercial stainless-steel alloys developed for high temperature use and are commercially available today, the rest of the materials of the project are not commercially available and they are not part of this job.

2. Description of the boilers

The materials have been exposed in two boilers with different fuels located in Grenoble and Biganos in France. The boiler in Grenoble is a waste-fired boiler while the boiler in Biganos is biomass-fired. In the waste boiler the materials where exposed for 1000 hours at 500 °C and 600 °C while the samples in the biomass boiler were exposed for 3000 hours at 500 °C and 600 °C. The samples in both Biganos and Grenoble were placed on metal probes and installed beneath the superheater region in the boilers. Figure 1 shows a picture of the probe with the sample rings on before the exposure. The probes are air-cooled with incorporated thermocouples connected to a PID (Proportional-Integral-Device) controller which enables regulation of the material temperature by regulating the flow of pressurized air.

Figure 1. Picture of the probe where the samples were attached

The sample matrix was different in each boiler. There were different samples because of the different needs of the two boilers, different ability to change the material as well as the companies economical situation. The differing ability is due to the differences in operation of the boiler.

Table 1. Samples in the boilers

Biomass boiler	*Waste Boiler*
P91	P91
AISI TP310H	AISI TP310H
Sanicro 28	13CrMo4-5
	Sanicro 28

2.1 Biomass boiler

The biomass boiler in Biganos is fueled by different types of biomasses, as previously stated, and can be seen in figure 2 below. The biomass used during the exposure was made up off waste wood, saw residue, bark and sludge from wood. The fuel is funneled in through the

bottom of the boiler where its immediately incinerated to create vapor. The vapor then rises to the superheater region where our samples were placed.

The steam parameters in the boiler during the sample exposure was:

Temperature: 520 °C
Pressure: 119 bar
Flow: 47 kg/s
Effect: 124 MW

The samples from the boiler in Biganos were exposed to the environment of the superheater region for 3000 hours at 500 °C and 600 °C. 3000 hours is a long probe exposure time for a boiler, the average operating time for a boiler each year is 8000 hours.

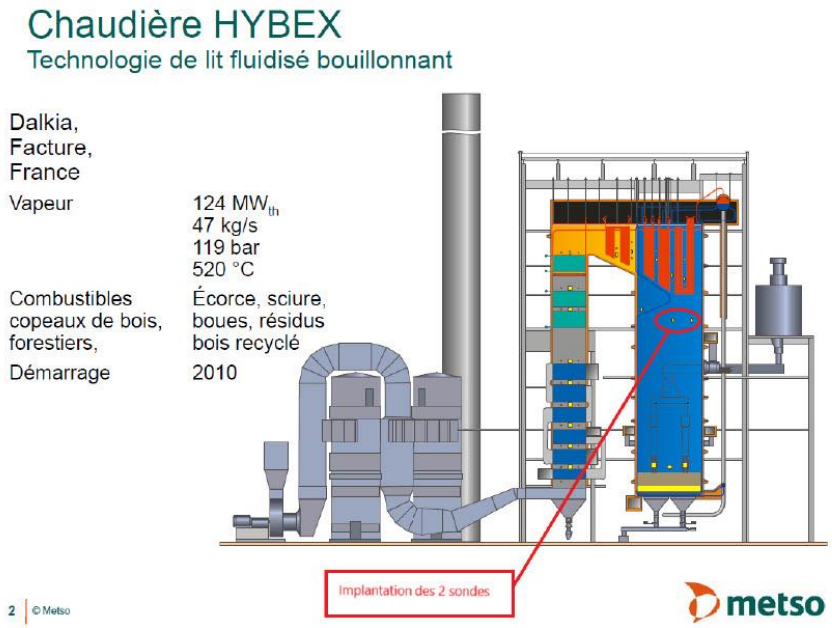

Figure 2. Schematic of the Biomass boiler in Biganos

2.2 Waste boiler

The boiler in Grenoble is waste-fired. The fuel is composed of waste wood, animal flour and coal. Similar to the biomass boiler the fuel for the waste material boiler is funneled in through the bottom and immediately incinerated to create flue gas. The flue gas then rises to where our samples are placed which is in the superheater region of the boiler. A schematic of the boiler can be seen below in figure 3.

When the samples were exposed in the boiler the fuel consisted of:

- 47 MW Waste wood
- 5 MW animal flour
- 18 MW coal

- Total: 70 MW

The samples in the boiler from Grenoble were exposed to the superheater environment of the boiler for 1000 hours at 500 °C and 600 °C. 1000 hours is 1/8 of the yearly operating time of an average boiler.

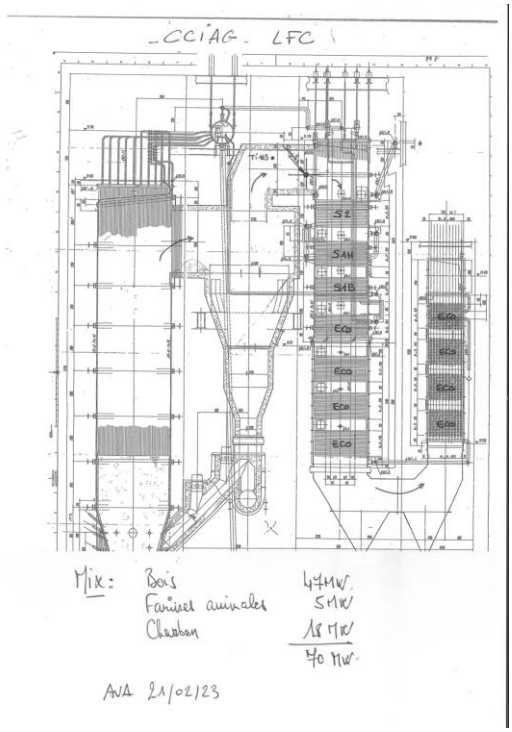

Figure 3. Schematic of the Waste boiler in Grenoble

3. Materials

Table 2. Percentage of elements in each metal sample

Elements (%)	P91	Sanicro 28	13CrMo4-5	AISI TP310H
Iron	89.55	36.8	98.3	53
Chromium	9	27	0.7-1.15	25
Nickel	0	31	0	20
Molybdenium	1	3.5	0.4–0.6	0
Manganese	0.3–0.6	≤2	0.4–1	≤2

The values in the table above are approximates and vary depending on supplier and which elements you choose to include. Apart from the listed elements there is also trace elements present, such as Vanadium, Silicone and Phosphorus.

3.1 P91

The steel alloy P91 consists of 9% Chromium and 1% Molybdenum as well as some other trace elements such as Carbon and Manganese, which increases the toughness of the metal. The carbon content increases the metals strength while Manganese enhances its ductility. The purpose of Chromium is to help resist oxidation at high temperatures by forming a protective oxide layer. Further Molybdenum also increases oxidation resistance as well as protection

from other forms of corrosion. P91 offers a good resistance to high temperatures due to its high Chromium content. This makes the alloy well suitable for use in for example boiler and superheater components. In terms of price, P91 is the second cheapest by amount of the 4 alloys analyzed.

3.2 Sanicro 28

Sanicro 28 is the most highly alloyed metal of the 4 with a composition of 27% Chromium, 31% Nickel, 3.5% Molybdenum as well as some other trace elements. This composition results in a highly corrosion resistant steel alloy, suitable for wet corrosive environments. One potential downside with Sanicro 28 is its limitation in use based on temperature. It limited to use in temperatures up to 550° C. One solution to this is to co-extrude the metal with a load carrier boiler tube to form a composite tube. By doing this you reduce thermal elongation and increase thermal transfer. Sanicro 28 has the highest price of the 4 steel alloys.

3.3 13CrMo4-5

13CrMo4-5 is a low alloyed steel with around 0.925% Chromium and 0.5% Molybdenum. This chemical composition constitutes to a high resistance regarding both corrosion and oxidation at high temperatures. The supplier temperature limitation is at 500°C. 13CrMo4-5 is the cheapest of the analyzed steel alloys.

3.4 AISI TP310H

AISI TP310H is a niobium stabilized nitrogen alloyed steel with 25% Chromium and 20 % nickel together with other trace elements. By stabilizing 310H, which is a high carbon alloy, with niobium and nitrogen you achieve an alloy with high temperature and creep resistance. This metal is suitable for environments with high temperature and corrosion. In corrosive conditions this steel can withstand temperatures from 525°C - 540°C and in non-corrosive environments up to 620°C. AISI TP310H is the second most expensive steel alloy.

4. Research method

In this project there were three main means of analysis the samples from the boilers. First the samples were prepared for analysis. Then they were observed with a scanning electron microscope (SEM) paired with energy dispersive x-ray spectroscopy (EDX). Lastly the coating deposit was analyzed with ion chromatography (IC).

4.1 Preparing sample

Before the samples could be analyzed they needed to be prepared to protect the coating deposit from falling off and to improve the cross section for enhanced observation. To protect the deposit all samples were sealed in epoxy and left harden for 1-2 days. After sealing the samples in epoxy, the remaining parts of the preparation was performed in sets of three samples each time due to the automatic grinder’s capability of polishing three samples at once.

When the epoxy had hardened the samples were removed from their containers and moved to a high-speed saw. The saw was used to cut all the samples individually into to two parts with equal size. Due to the saw being continuously being sprayed with water-free oil to protect it from overheating the samples became covered with oil and needed to be cleaned. The samples where then cleaned with acetone. Once the samples were clean, they were manually grinded on the opposite side of which would be observed in the SEM to expose the metal and thus enabling conduction of electrons. When the metal had been exposed the samples were placed in the holder of the automatic grinder and polished with varying grit of grinding paper, the paper varied between 800 grit – 4000 grit.

This process was the repeated for all 11 samples for a total of 4 session in the prep lab. When all samples were done an unexposed 13CrMo4-5 sample was also cut to be used for calculating the thickness of the metal before being exposed to the boilers.

4.2 Scanning Electron Microscope/Energy-dispersive X-Ray spectroscopy

The first analysis that was done on the prepared samples was to see how much of the metal that had been lost during their exposure in the boilers. The cross sections of the sampels were analysed by means of scanning electron microscopy (SEM) and energy dispersive X-ray (EDX) with an accelerating voltage of 20 kV using an FEI Quanta 200 equipped with an Oxford Instruments XMaxN 80 T EDX detector. The thickness of the rings after exposure was measured at eight locations in similar positions as before exposure to evaluate the material loss. This is illustrated under section 5.2 as graphs.

After analyzing the metal, oxide layer and coating deposit using SEM either one or two points on the sample was chosen and analyzed further using Energy-dispersive X-Ray spectroscopy. Using EDX, both “map” and point analysis was acquired. A “map” analysis is an examination of composition of the whole samples while point analysis is the analysis of a specific point in the sample. From this data it was possible to observe concentrations of different atoms in different places on the sample, in other words the atomic composition in both oxide layers and coating deposits. To calibrate and make sure that the EDX software was working properly a point analysis of the metal surface was made. The acquired percentage values of atomic composition were then compared to standard values from the supplier. The program used for EDX was Aztec from Oxfords Instruments.

4.3 Ion Chromatography

Ion chromatography was used to analyze the composition of the coating deposit that formed on the exterior of the samples in the two different boilers. The coating that is created depends on which fuel is used in the boiler and at what temperature the boiler operates at, this means that the different types of metal do not affect the composition of the deposit. This analysis is done to determine what substances cause the corrosion in the boilers and how the two boilers differentiate from each other. Because of the metal not affecting the composition of the deposit its only necessary to have a sample for each boiler and temperature. The result is 4 samples:

- Biomass boiler at 500 °C
- Biomass boiler at 600 °C

- Waste boiler at 500 °C
- Waste boiler at 600 °C

The process for preparing the samples for ion chromatography was the same for the deposit from the two boilers. The coating was broken off from the metal samples from each boiler. The deposit from each sample was then crushed individually until it lost its rocklike properties and took on more of a sand like aspect. The deposit coating was then mixed with 500 ml of deionized water in a marked graduated flask for a total of 4 different flasks. A sample of 5 ml was the taken from each flask and added to an IC vial. The vials were then put into the IC with standard samples for SO_4 and Cl and deionized water. These standard samples contained different amounts of substance/L. The ion chromatography (IC) is a Dionex ICS-90 system. The anions were analyzed with an IonPac AS4ASC analytic column and 1.8mM NaHCO3/1.7mM NaHCO3 was used as solvent. The flow rate was 2ml/min.

Table 3. Standard samples of SO4 and Cl

SO_4	Cl
50 mg/L	10 mg/L
100 mg/L	50 mg/L
250 mg/L	100 mg/L
500 mg/L	250 mg/L
750 mg/L	
1000 mg/L	

The standard samples for Cl contained less mg/L then SO_4 because of observations made during SEM (EDX) where it showed low amounts of Cl in the deposit, so it was determined that there would not be high amounts of Cl in the deposit. The chromatography was then started and left to run its course, once the process was done the results were noted down.

5. Result and Discussion

In this part of the study the data and images of the SEM, EDX and IC analysis will be presented.

5.1 Scanning Electron Microscope images and EDX data

The following section will present the images created by SEM of the eleven different samples. For an easier reading experience the samples have been divided in 4 different main categories:

- Biomass 500 °C
- Waste 500 °C
- Biomass 600 °C
- Waste 600°C

The oxide layer that is created on the surface of the samples depends on several factors, such as if the sample is directed directly towards the vapor from the burning of the fuel, the compounds that are present in the vapor and the temperature of the vapor. The images shown here are the average appearance of each sample.

This section will also present the data from the EDX analysis of each of the samples. The EDX “mappings” and point analysis shows a clear pattern, that there is close to no chlorine in the coating deposit of the samples. This is also proven during the IC analysis where the amount of chlorine in the deposit was shown to be extremely low. The “maps” show that the low amount chlorine is true for all the different samples. The lack of chlorine in all the samples is a result of the fuel used in the boilers, for if the fuel contains chlorine so will the deposit that forms on the samples. The fuel used in the boilers is mainly wood, biproducts of wood production and animal flour which are all products that are chlorine free.

5.1.1 Biomass 500 °C Samples

This section contains the SEM images and the EDX data of the samples from the biomass boiler at 500 °C.

5.1.1.1 P91

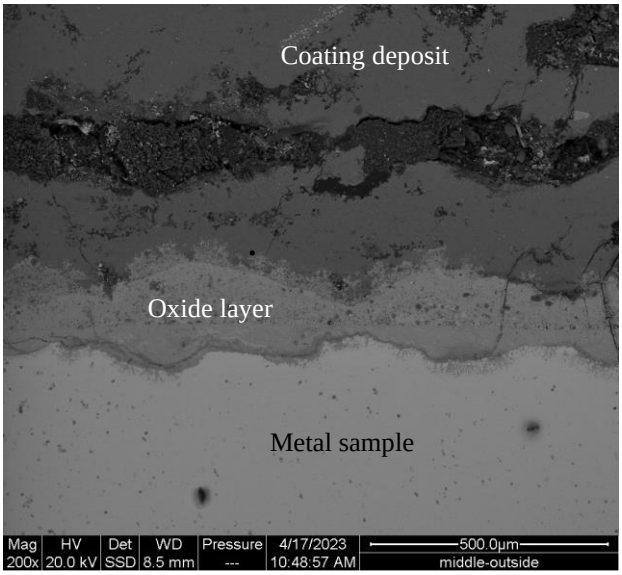

Figure 4. SEM image of P91 sample from Biomass boiler at 500 °C

The P91 sample can be seen in figure 4 and is shown to have a clear oxide layer that is winding through the metal. The oxide scale is made composed of an Fe-rich outward growing oxide and a Fe-Cr rich inward growing spinel oxide. The oxide scale is wider than the other samples, these can be seen below in figure 5 and figure 6. The composition of the oxide scale is confirmed by the EDX data below in figure 5.

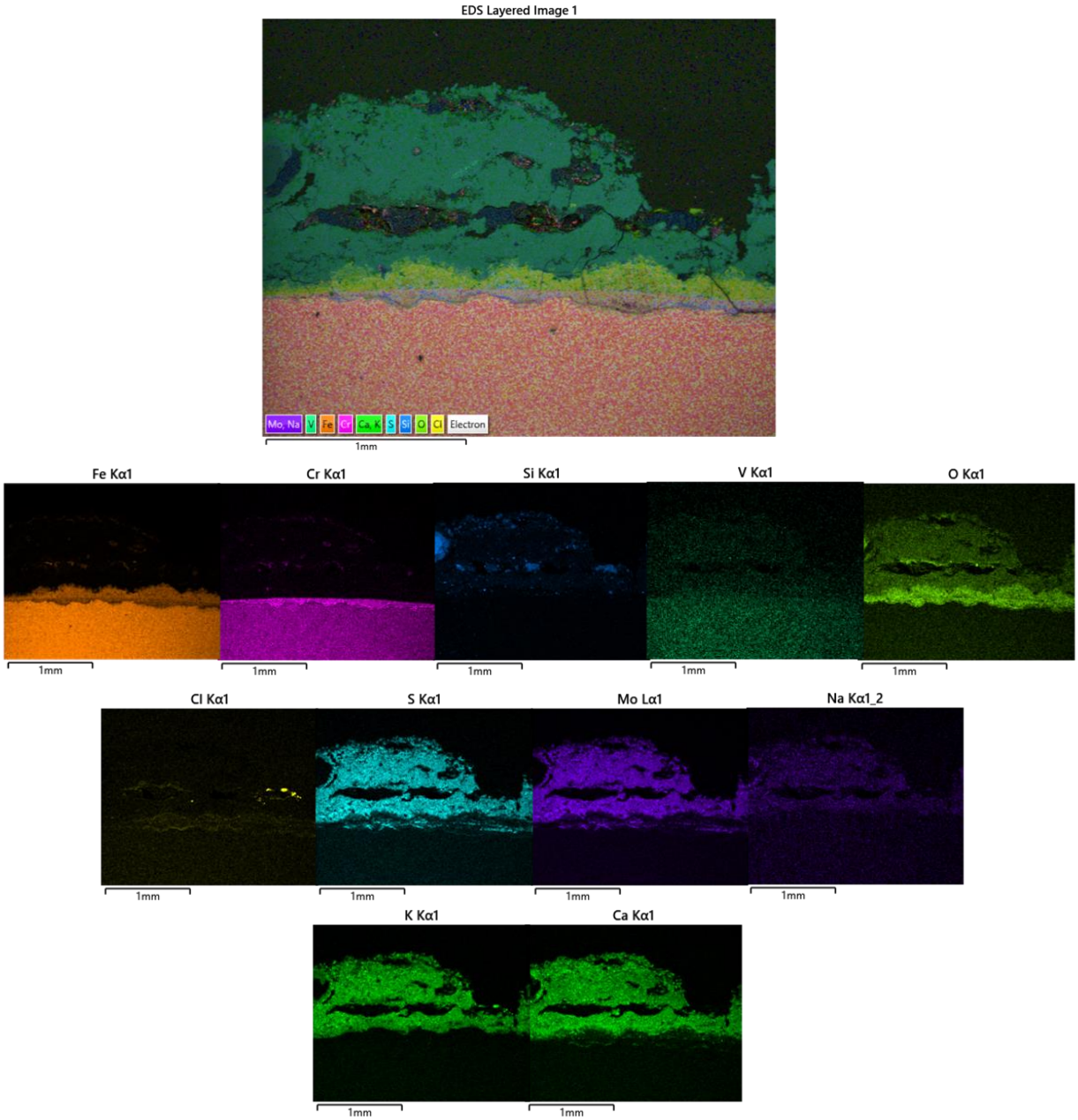

Figure 5. EDX map of P91 at 500 °C in the biomass boiler

The “map” of the P91 samples shows that the metal only consists of Iron and chromium which matches with the given data for the metal, there is also trace amounts of vanadium. It also shows that the majority of the oxide layer that was created during the exposure is an iron oxide while a small part of the oxide is made up of chromium. The iron oxide can be seen growing both outwards from the metal as well as inwards into the metal, while the chromium is only detected inwards. The oxide map of the sample also shows a clear oxide layer.

The coating deposit is as predicted nearly chlorine free, there only exists small “islands” of chlorine in the mappings but they are not large enough to create any impactful amounts of chlorine. Instead, the majority of the deposit is made up of potassium, calcium, sulfur and small amounts of sodium. There is also trace amounts of molybdenum in the deposit as well as traces of silicon. The trace of silicon most probably comes from the preparation of the samples where the grinding papers contain silicon, while the molybdenum comes from the

metal and was broken off during the grinding of the sample. The remaining elements comes from the wood that was used as fuel in the boiler.

5.1.1.2 Sanicro 28

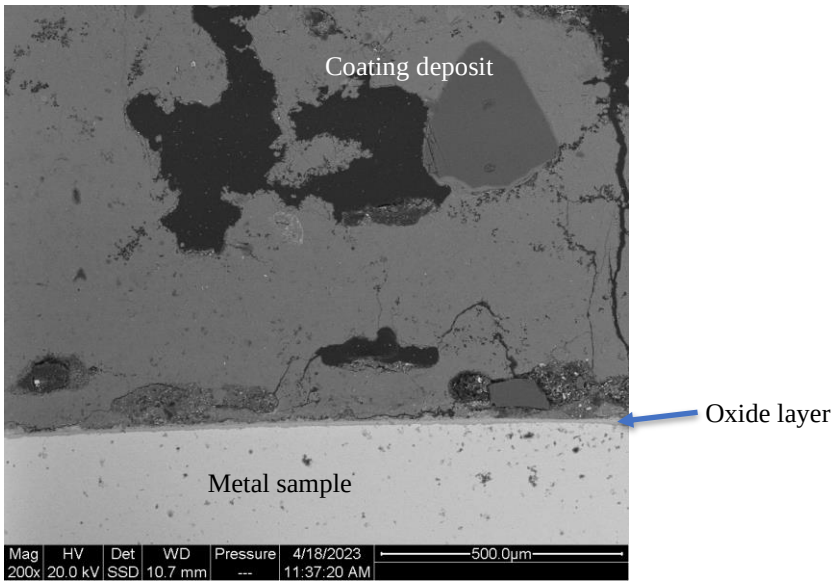

Figure 6. SEM image of Sanicro 28 sample from Biomass boiler at 500 °C

Figure 6 shows the SEM image of the Sanicro 28 sample from the biomass boiler, this samples has a barely visible oxide layer. When comparing the oxide layers of P91 and Sanicro 28 it is easy to see that Sanicro 28 has a much straighter layer which point towards it being more chromium rich than the P91 layer. The EDX analysis below in figure 7. And figure 8. show that the oxide layer is made up of chromium oxide with a small part being iron oxide.

The EDX analysis of Sanicro 28 consists of two mappings because of the small oxide layer which was hard to capture while simultaneously analyzing the coating deposit. Map 2 is created with enhanced magnification and focused on a different part of the sample where the oxide layer was larger.

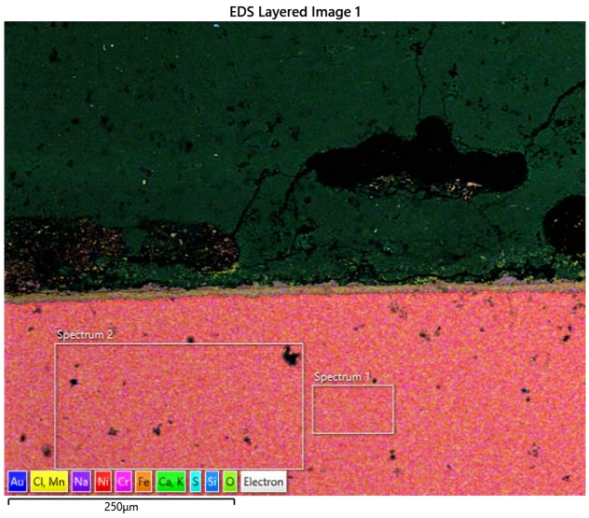

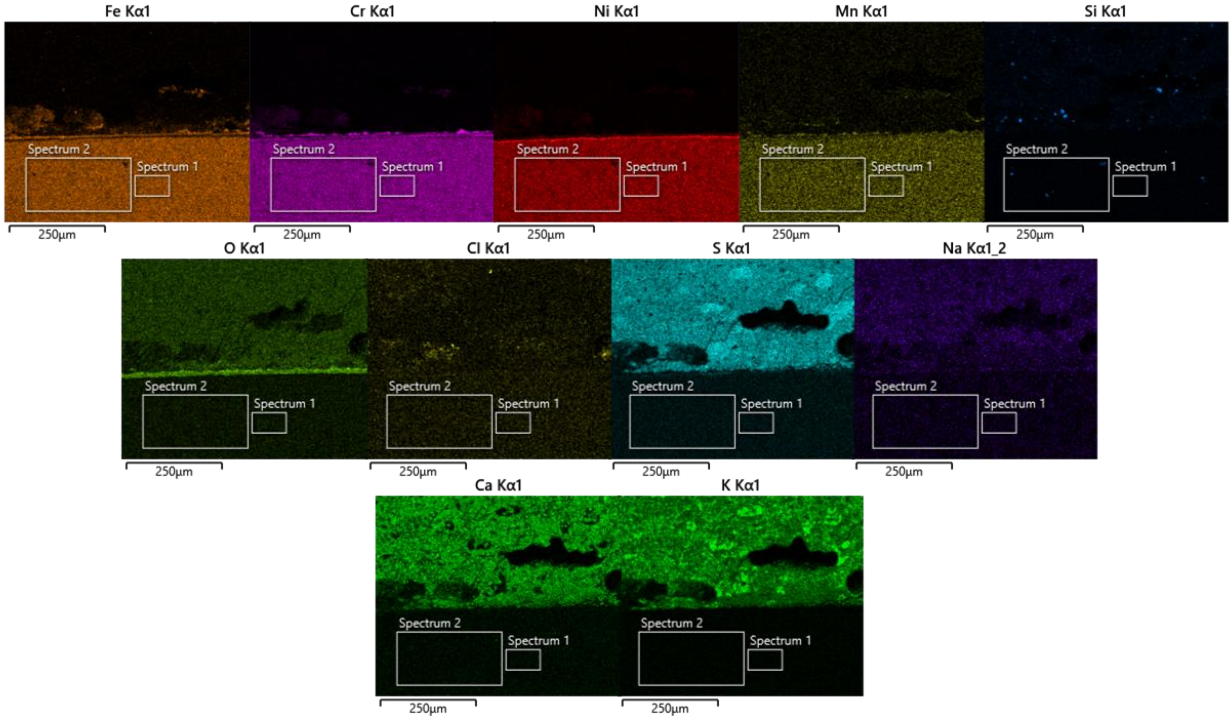

Figure 7. EDX map 1 of Sanicro 28 from Biomass boiler at 500 °C

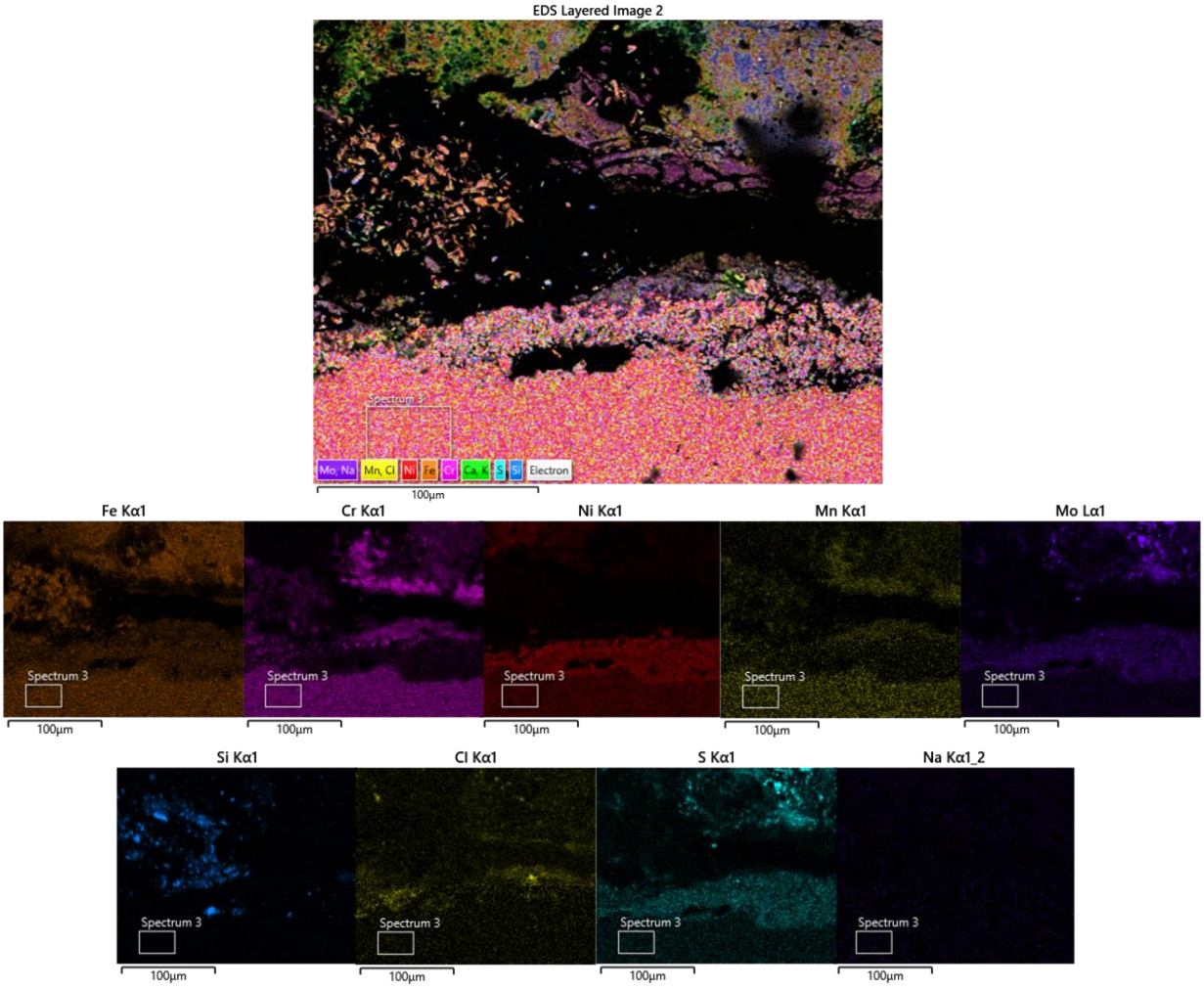

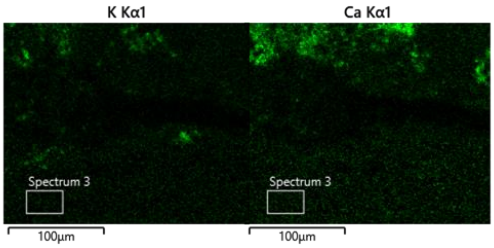

Figure 8. EDX map 2 of Sanicro 28 from Biomass boiler at 500 °C

In the first mapping of Sanicro 28 the maps show that the metal is made up of iron, chromium, nickel, and manganese. The oxide layer from map 1 is thin which makes it hard to observe which of the metals that have oxidized, this can however be seen in map 2 where the magnification is enhanced, and the oxide layer is shown more clearly. The second map clearly shows oxide scale is composed by a inward growing Ni-rich oxide with a Fe-Cr oxide on top. The oxide layer on the Sanicro 28 sample is the thinnest of the three samples from the 500 °C biomass boiler. The thin layer is still outwards and inwards growing but thanks to nickel the growing process is slow. Unlike the P91 sample the two oxide layers differ in composition, the outward growing oxide consists of iron and chromium and the inwards growing oxide consists of iron, chromium and nickel. The nickel gives an improved protection from oxidization then Iron because nickel oxide is more compact and stops oxygen from reacting with the metal surface.

The pattern of low amounts of chlorine is followed by Sanicro 28s deposits as well. The deposit of the samples contains sulfur, potassium, oxygen, sodium, and calcium. Both the Sanicro 28 samples deposit and the P91 samples deposit are composed of the same elements because they were exposed to the same boiler during the same period. There are also trace amounts of silicon in the deposit as a result of the preparation of the samples when the grinding papers with silicon were used.

5.1.1.3 AISI TP310H

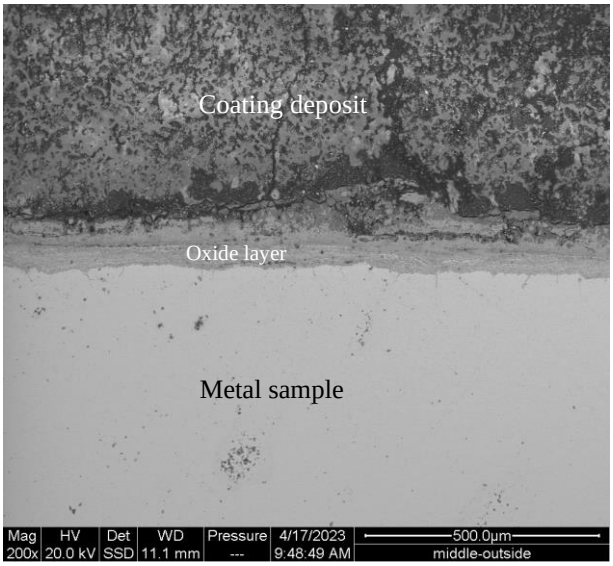

Figure 9. SEM image of AISI TP310H sample from Biomass boiler at 500 °C

In Figure 9. the AISI TP310H samples is presented. The oxide layers is thinner than in P91 but wider than Sanicro 28. The AISI TP310Hs oxide layer is straight and well adheared to the surface so it can be presumed that is contains high amounts of chromium, this can be seen in the EDX “map” of tha sample below in figure 10.

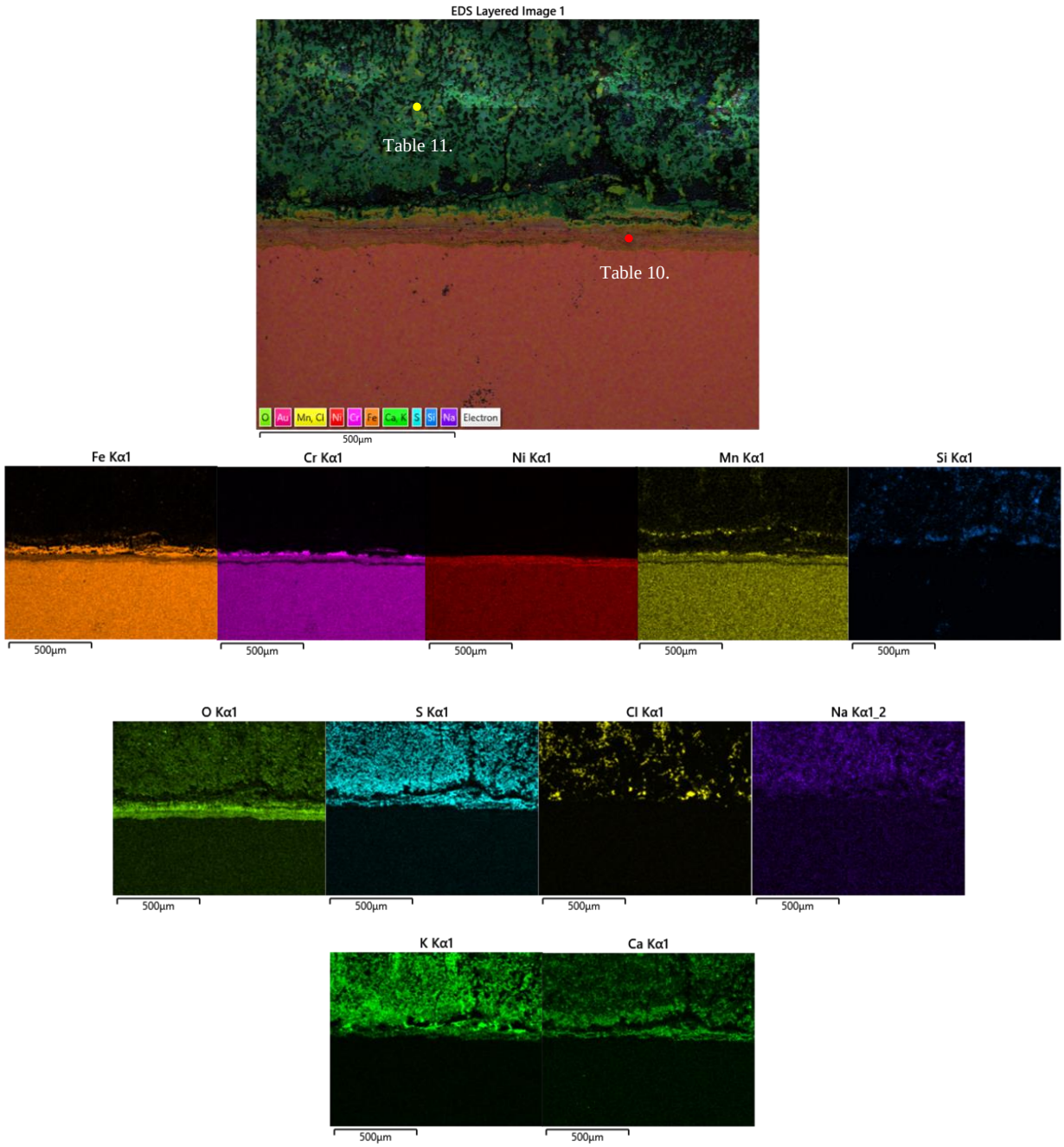

Figure 10. EDX map of AISI TP310H from Biomass boiler at 500 °C

The map of the AISI TP310H sample shows that the metal is made up of mostly iron, chromium, nickel and manganese. These are the metals that should make up the sample according to the supplier. The oxide layer is thinner than the layer in P91 and wider than the layer from the Sanicro 28 sample, this indicates that TP310H’s oxide layer give greater protection the layer from the P91 sample but inferior protection than the layer from the Sanicro 28 sample. Similar to the Sanicro 28 sample the outwards growing oxide in the

TP310H samples can be seen only consisting of chromium and iron oxide while the inwards growing oxide consists of iron, chromium, and nickel oxide.

Such as the other samples from the 500 °C biomass boiler the deposit of the TP310H sample contains low amounts of chlorine and the same elements as the two other samples from the biomass boiler.

Table 44. Amount of each element in a specific part of the sample (See figure. 10)

Elements	Weight %
O	18,17
Na	0,09
Si	1,22
S	0,06
Cl	0,49
K	0,16
Ca	0,04
Cr	37,74
Fe	22,54
Ni	19,49
Total	100

Table 10 illustrates a more detailed overview of the weight composition of AISI TP310H. According to the table there is clear evidence of a relatively pure protective oxide layer consisting of iron, chromium and nickel.

Table 55. Amount of each element in a specific part of the sample (See figure. 10)

Elements	Weight %
O	36,25
Na	0,18
Si	0,15
S	27,18
Cl	0,19
K	17,97
Ca	17,96
Cr	0,07
Fe	0,06
Ni	0,01
Total	100

Table 11 displays the weight percentages in the deposit layer of the sample. There is a clear difference in the oxide layer. For example, there are little to no traces of iron, chromium and nickel. Instead, there is relatively high concentration of calcium, potassium and sulfur.

5.1.2 Waste 500 °C Samples

This section contains the SEM images and the EDX data of the samples from the waste boiler at 500 °C.

5.1.2.1 P91

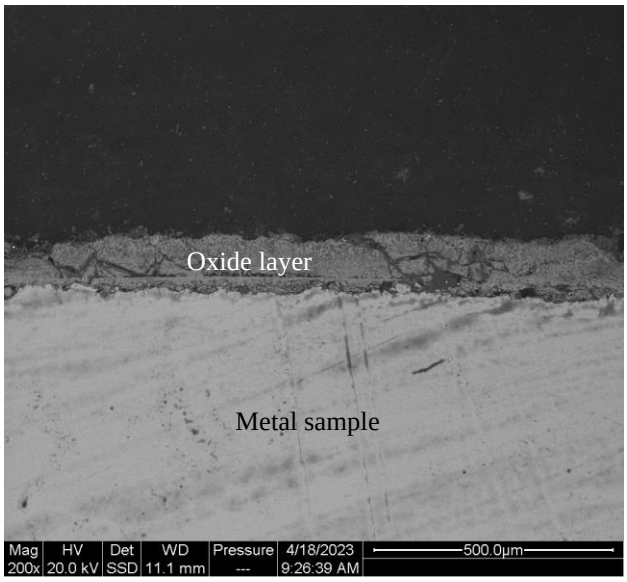

Figure 11. SEM image of P91 sample from Waste boiler at 500 °C

The most distinct feature of P91 samples in Figure 11 is that it lacks coating deposit. The lack of deposit is most likely due to spallation during the sample preparation. Except for the lack of deposit the P91 waste samples oxide layer is straighter then the P91 biomass layer, this is probably because of the shorter exposure time for the waste samples.

The second mapping of the P91 sample from 500 °C was due to the interesting patterns in the deposit and oxide layer.

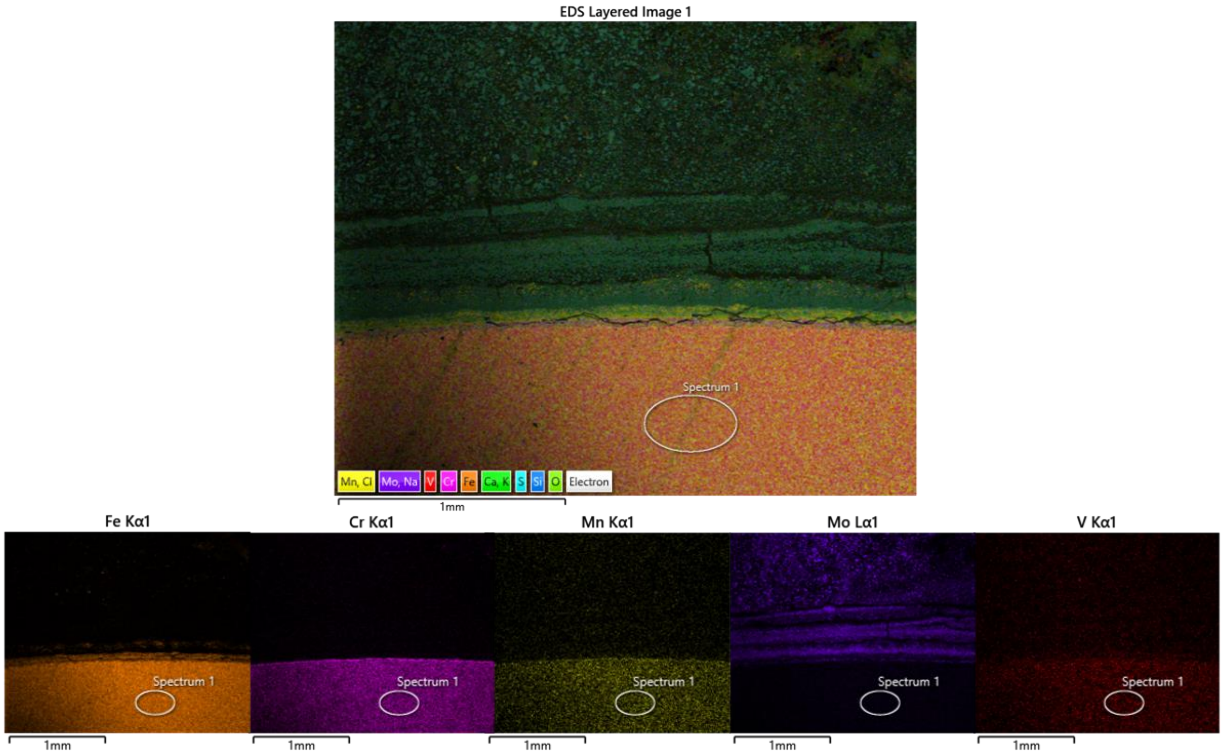

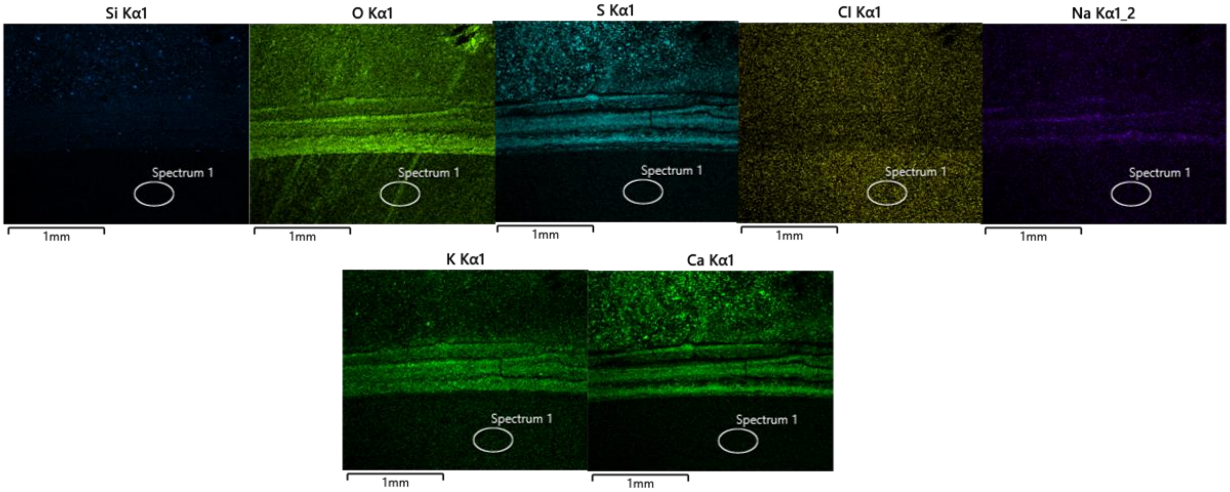

Figure 12. EDX map 1 of P91 from Waste boiler at 500 °C

Table 13.

Table 12.

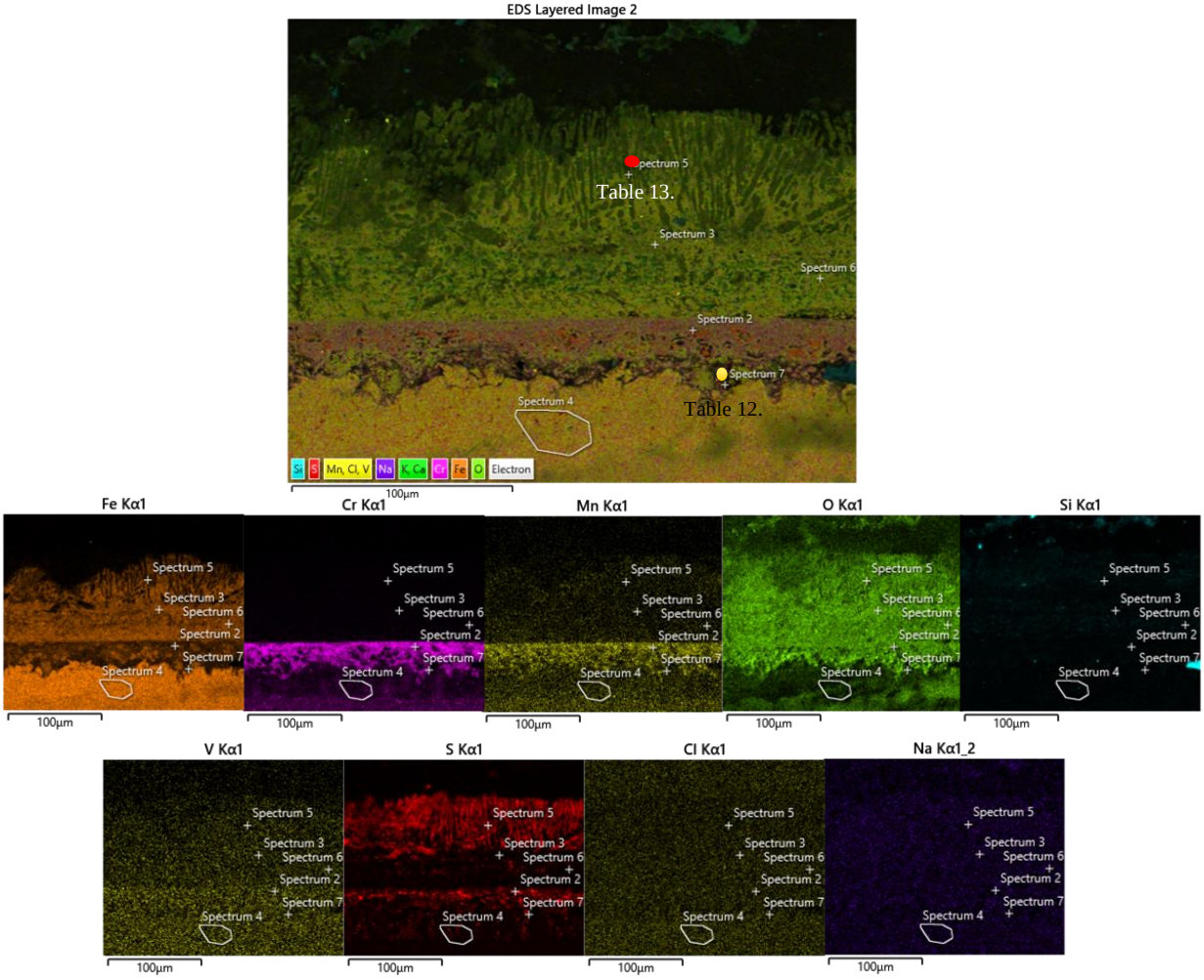

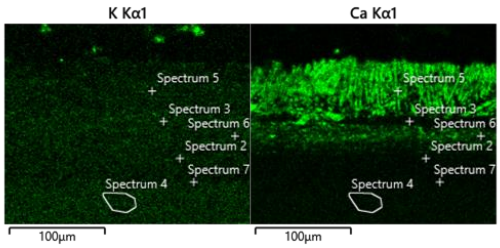

Figure 13. EDX map 2 of P91 from Waste boiler at 500 °C

In the case of P91 in the waste boiler there are two vastly different mappings. On the first mapping there is a smooth line of thin Iron oxide that to some extent protects the metal. Together with this, there may be a small amount of Fe-Cr oxide present as well. Elements noticeable in the deposit are calcium, potassium, sodium and sulfur which originate from the fuel. Small amounts of molybdenum as well as silicone, from grinding, is also present

The first map shows the sample that was placed on the shadow side. In other words, the shadow side is not exposed to the same high force of flue gas as the wind side shown in mapping number 2. Because of this there is more aggressive oxidation and corrosion. From the mapping it is possible to distinguish both outward but also inward growing oxide. The main form of protective oxide is inward growing chromium oxide. There is clear evidence that the high pressure from the corrosive boiler gas impacts the oxide layer's ability to withstand corrosion. This is noticeable because some iron has begun to corrode away and both small and big cracks are present. Map 2 and map 1 has similar deposit elements, except for no sodium illustrated in mapping 2.

Table 66. Amount of each element in a specific part of the sample (See figure. 13)

Elements	Weight %
O	29,7
Na	0,22
Si	3,03
S	0,84
Cl	0,05
K	0,07
Ca	0,03
V	1,04
Cr	26,9
Fe	28,87
Ni	0,03
Mo	9,53
Total	100

Table 12 provides data regarding the weight composition of the oxide layer of P91. The main elements are iron oxide and chromium oxide.

Table 77. Amount of each element in a specific part of the sample (See figure 13.)

Elements	Weight %
O	49,9
Na	0,27
Si	5,29
S	8,06
Cl	0,09
K	0,7
Ca	11,15
V	0,04
Cr	0,00
Fe	24,51
Ni	0,00
Mo	0,00
Total	100

Table 13 is a compilation of weight composition of the outer deposit layer of P91. Many different elements are present in the deposit such as sulfur, calcium and potassium. The fact that there is a lot of iron oxide present this far out in the deposit indicates a poor protective oxide layer together with many cracks as can be seen in figure 13.

5.1.2.2 13CrMo4-5

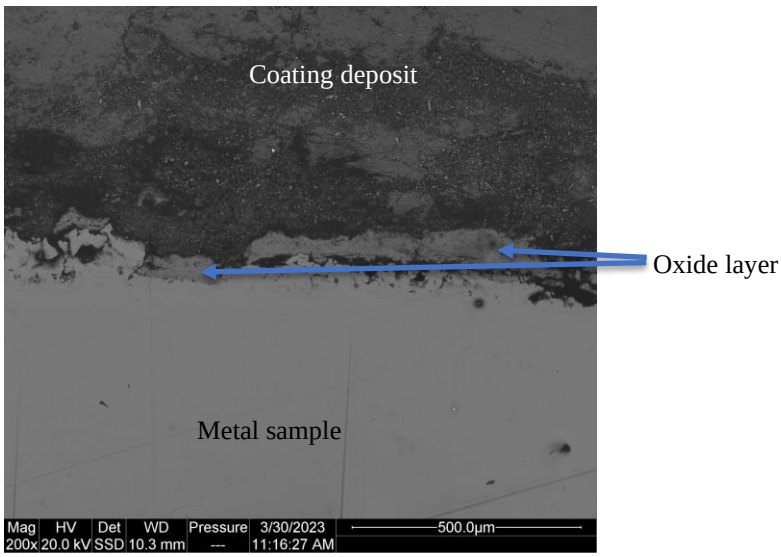

Figure 14. SEM image of 13CrMo4-5 sample from Waste boiler at 500 °C

Figure 14 shows that the 13CrMo4-5 is cracked along the edges and it presents a non-protective fractured oxide layer. These are both signs of poor corrosion protection. The 13CrMo4-5 sample has a less protective oxide layer and edge than the P91 sample, which means that P91 will have a longer lifespan then 13CrMo4-5.

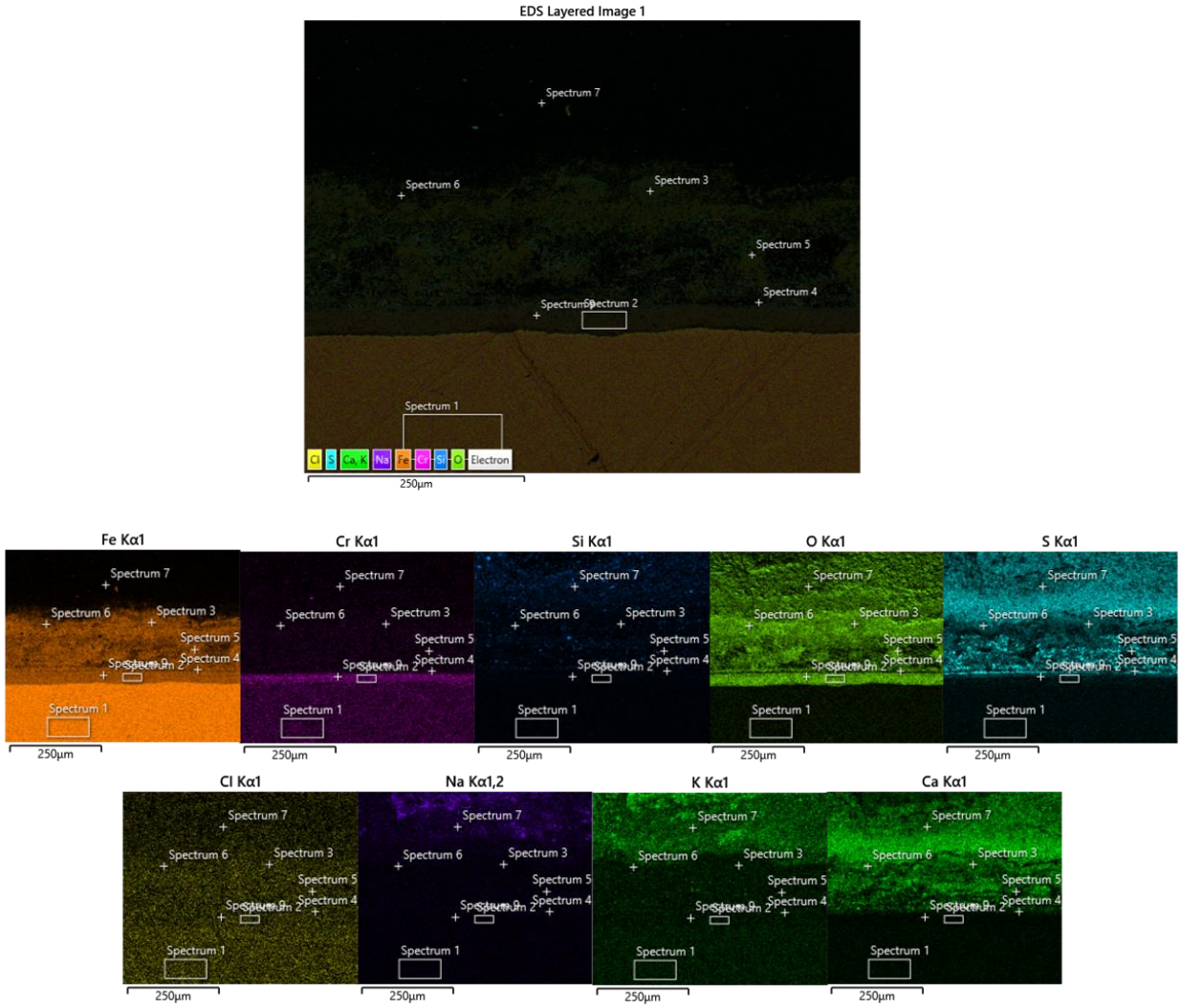

Figure 15. EDX map 1 of 13CrMo4-5 from Waste boiler at 500 °C

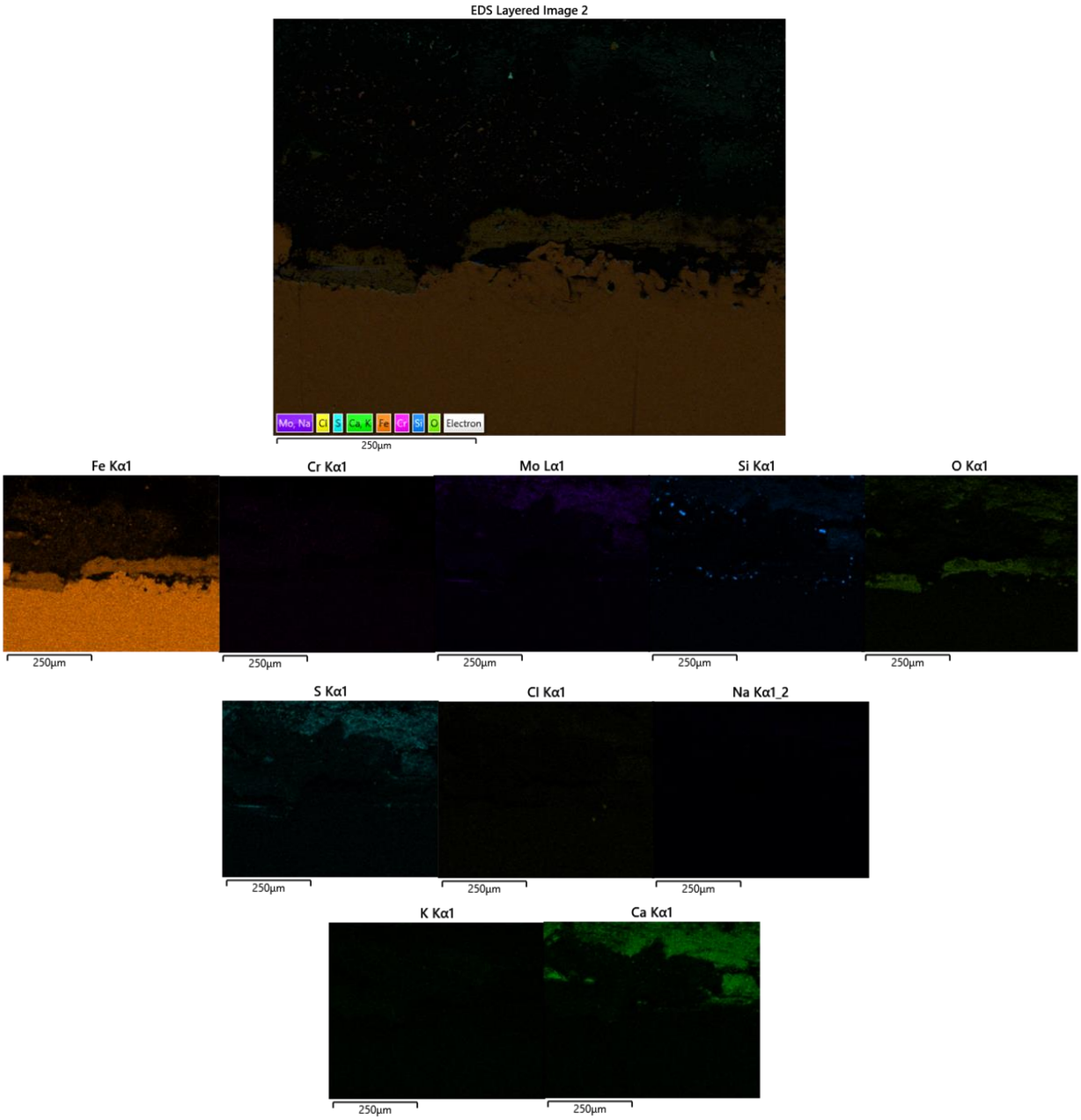

Figure 16. EDX map 2 of 13CrMo4-5 from Waste boiler at 500 °C

Just as P91, 13CrMo4-5 has two mappings. One of the flue gas side and one of the shadow side. The is a clear difference in both corrosion rate and deposit layer depending on side. The first mapping shows a clear and wide oxide layer with a fixed deposit layer attached. This would indicate that this is the shadow side. The oxide layer consists of mainly chromium and iron oxide. Unfortunately, the mapping of molybdenum is missing from this analysis. However, sulfur and molybdenum can be mixed up in the EDX machine. Therefore, the strong indication of sulfur especially in the oxide layer would indicate some molybdenum oxide. The deposit layer consists of sulfur, sodium, potassium and calcium.

Mapping number 2 of the flue gas side shows a more brittle and winding oxide layer. Because of the low-quality strength and protection it offers, it has fallen off because of the pressure of epoxy when hardening. This indicates that this steel alloy is not corrosion resistant enough. There is no attached deposit layer to the metal, although some calcium,

molybdenum and sulfur can be detected. One probable reason for this is probably that the strong forces from the flue gas impedes gas particles from forming a deposit layer.

5.1.2.3 AISI TP310H

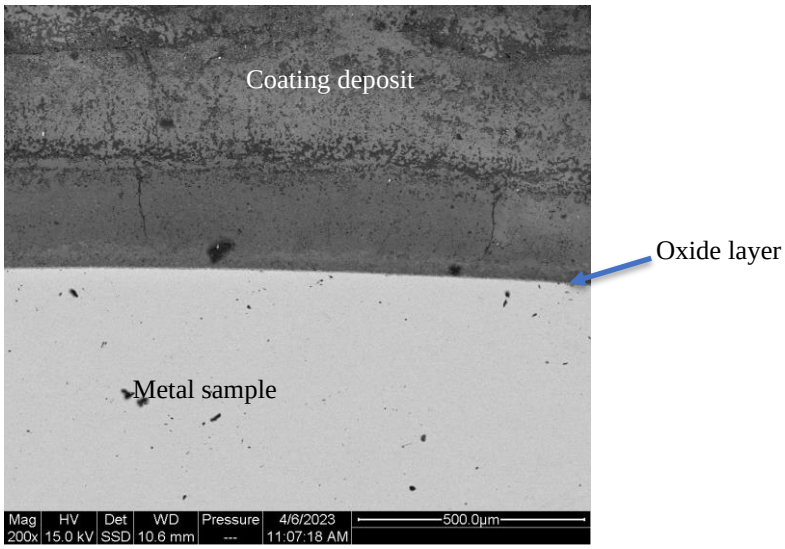

Figure 17. SEM image of AISI TP310H from Waste boiler at 500 °C

The AISI TP310H sample from the waste boiler can be seen in Figure 17. The image shows a thin and straight oxide layer, similar to the sample from the biomass boiler of the same alloy. Out of the three exposed metals in the waste boiler, it is clear that AISI TP310H has the highest corrosion resistance probably due to its high amounts of chromium.

Similar to the Sanicro 28 sample from the 500 °C biomass boiler the oxide layer of AISI TP310H from the 500 °C waste boiler was thin, so a second mapping was made with enhanced magnification for better observation.

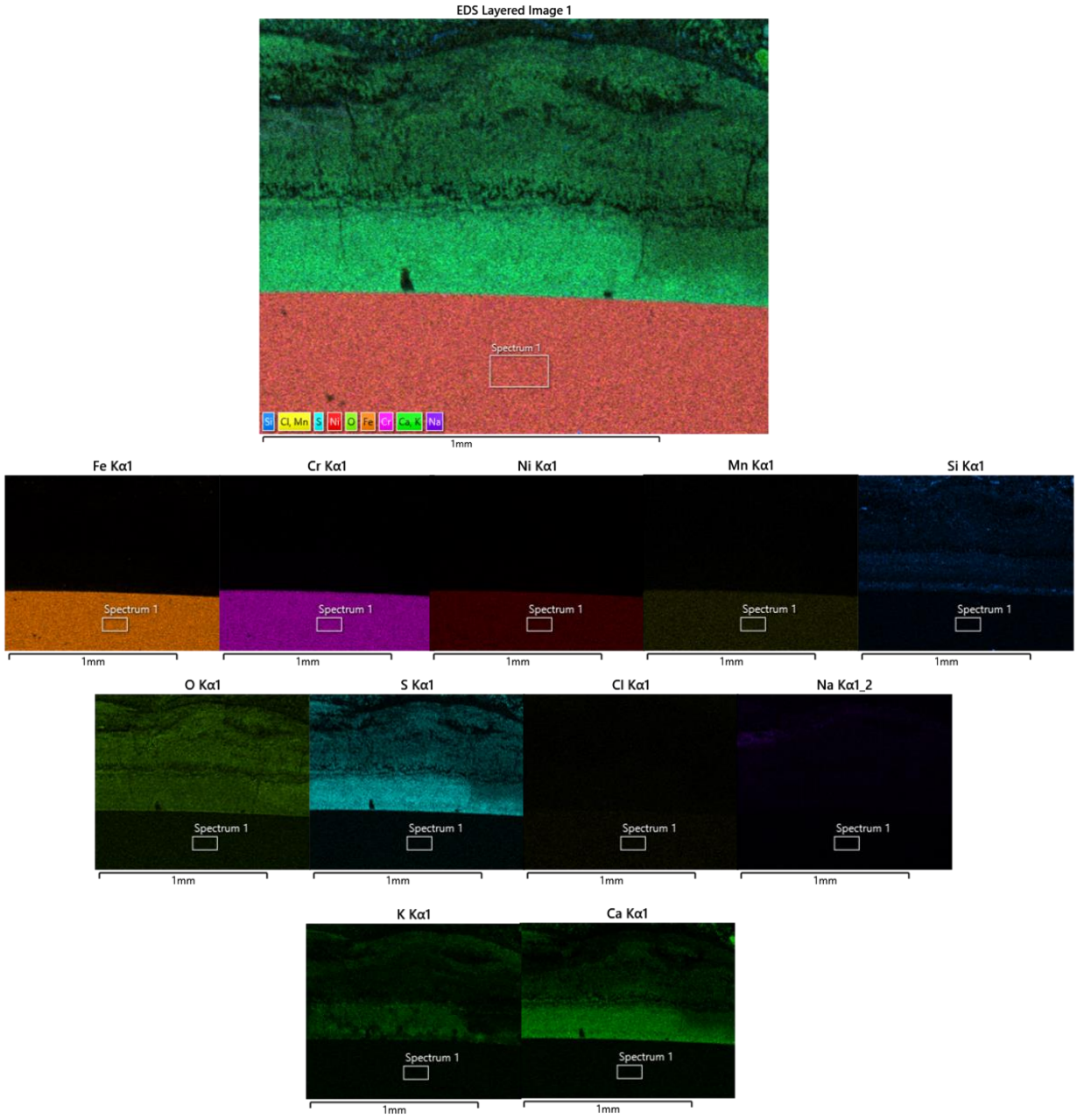

Figure 18. EDX map 1 of AISI TP310H from Waste boiler at 500 °C

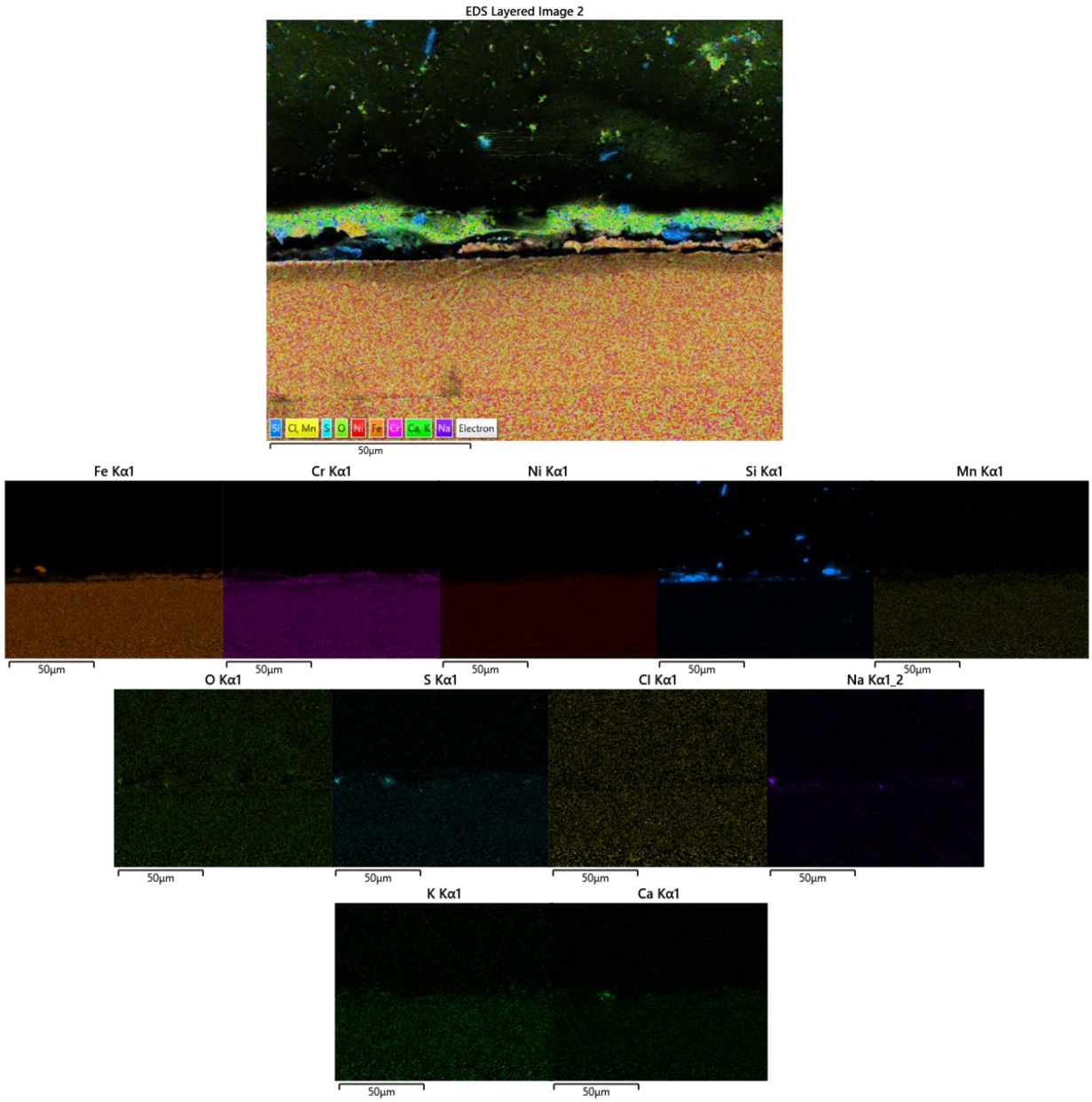

Figure 19. EDX map 2 of AISI TP310H from Waste boiler at 500 °C

The oxide layer of the AISI TP310H samples is the thinnest of all the samples from the waste boiler. Its layer is so thin that with increased magnification its still difficult. This thin layer is evidence that AISI TP310H is the most corrosion resistant material out of the ones tested in the waste boiler, its high resistance to corrosion comes from the high concentration of nickel and chromium in the alloy. Even though the oxide layer cannot be seen in the EDX mappings it still exists, as can be seen in the result of the SEM analysis of the sample.

The deposit of the ASISI TP310H samples consists of the same material as the other samples that were exposed to the waste boiler at 500 °C.

5.1.3 Biomass 600 °C samples

5.1.3.1 P91

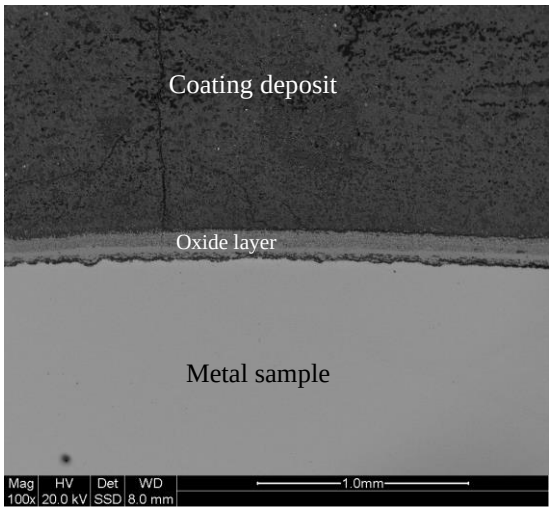

Figure 20. SEM image of P91 from Biomass boiler at 600 °C

When comparing the P91 in figure 20 from 600 °C biomass boiler to the P91 sample from 500 °C biomass boiler, it can be seen that the oxide layer of the 600 °C sample is straighter and smoother than the 500 °C sample. This can be because of several reasons, the different magnification of the images or which side of the sample the image was created from etc.

5.1.3.2 Sanicro 28

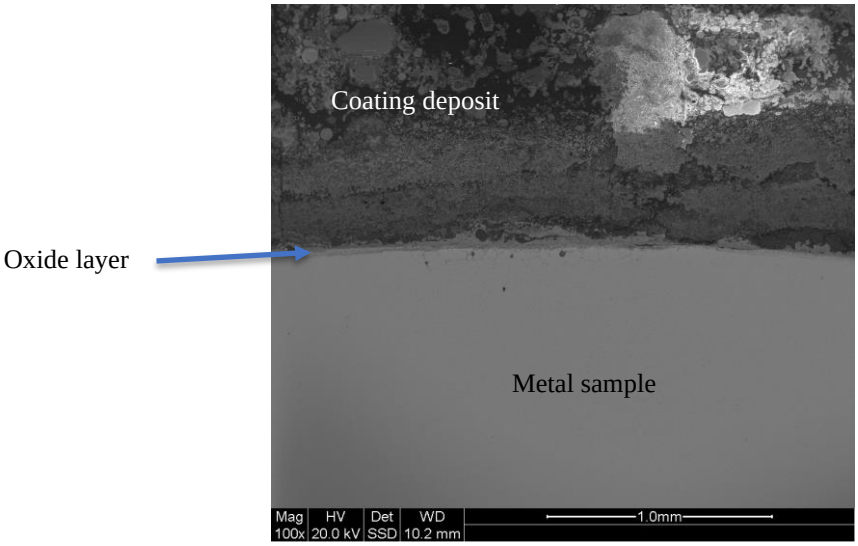

Figure 21. SEM image of Sanicro 28 from Biomass boiler at 600 °C

In figure 11 the Sanicro sample from 600 °C in the biomass boiler can be seen to have a wavier oxide layer then the Sanicro sample from 500 °C biomass boiler. Unlike the 500 °C biomass sample the 600 °C sample has many outcropping in its oxide layer, as well as its being more uneven across its surface.

5.1.3.3 AISI TP310H

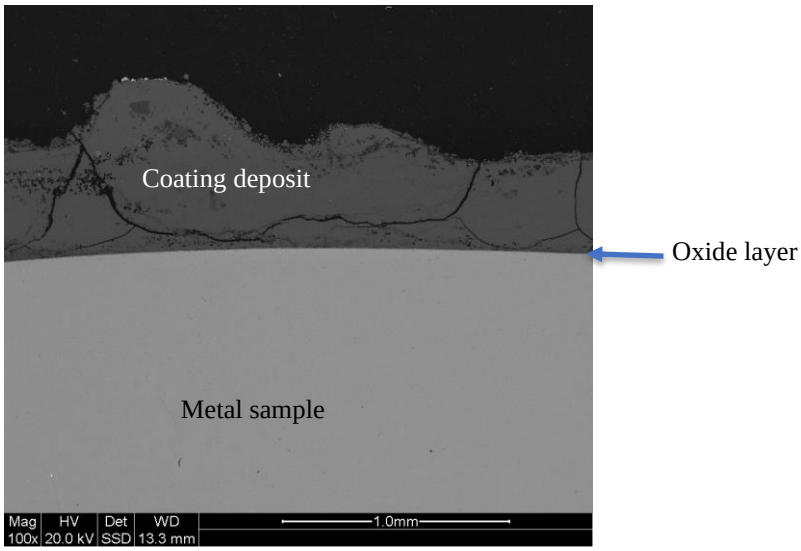

Figure 22. SEM image of AISI TP310H from Biomass boiler at 600 °C

The AISI TP310H sample from 600 °C can be seen in Figure 12 where it has a barely visible oxide layer. It can thus be presumed that a low amount of metal has been lost.

5.1.4 Waste 600 °C Samples

This section contains the images of the samples from the Waste boiler at 600 °C.

5.1.4.1 Sanicro 28

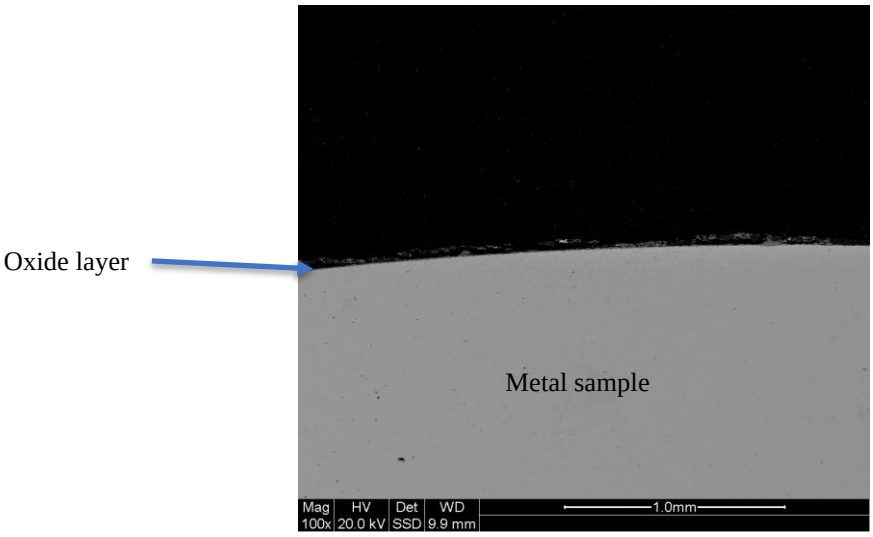

Figure 23. SEM image of Sanicro 28 from Waste boiler at 600 °C

Figure 13 shows Sanicro 28 after 1000h int the waste boiler at 600 °C and similar to the AISI TP310H sample from 600 °C in the biomass boiler it has a barely visible oxide layer.

5.1.4.2 AISI TP310H

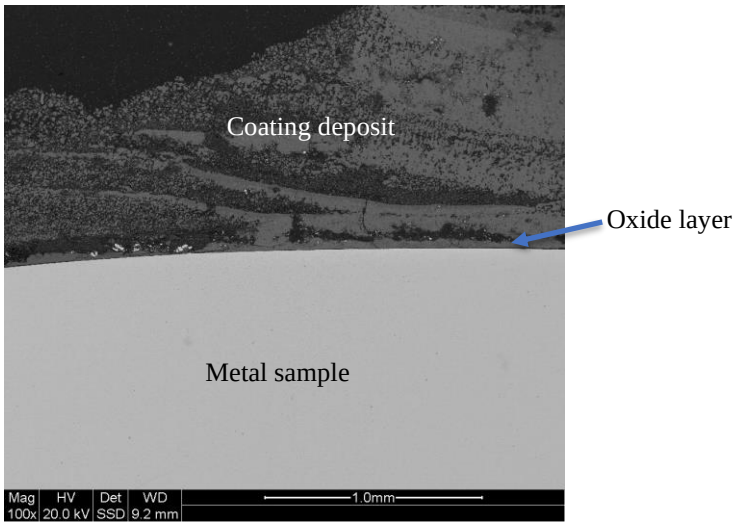

Figure 24. SEM image of AISI TP310H from Waste boiler at 600 °C

The AISI TP310H sample at 600 °C from the waste boiler is depicted in figure 14, where it can be seen to have a small oxide layer that is thicker than the layer of Sanicro at 600 °C from the waste boiler.

5.1.5 EDX data for 600 °C samples

Due to insufficient time, there not being a need and the service in the SEM/EDX equipment no mappings were created for the 600 °C samples. There was no need for EDX of the 600 °C samples because they were exposed to the same boiler as the 500 °C jus at a higher temperature, the deposit is there for equivalent to the deposit of the 500 °C samples as the corrosion mechanics are the same for the two temperatures.

5.2 Material Loss of samples

In this section the material loss of all ten samples will be presented and discussed.

5.2.1 Biomass boiler samples at 500 °C

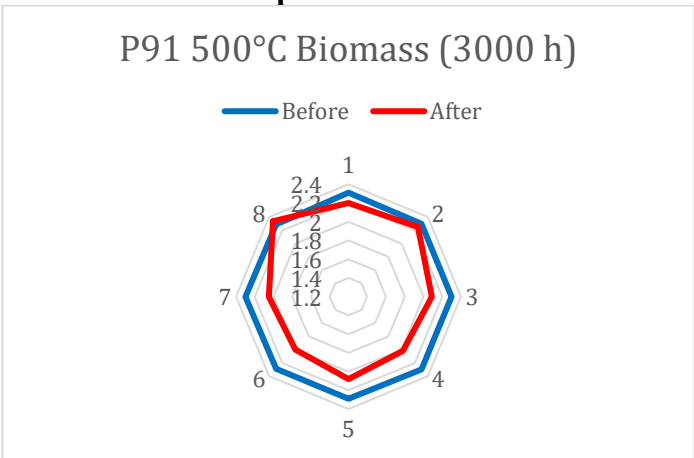

Figure 25. Material loss of P91 in Biomass boiler at 500 °C after 3000h

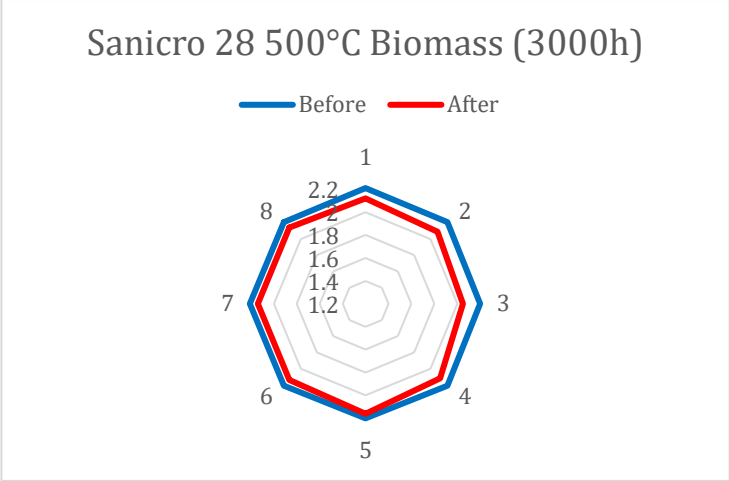

Figure 26. Material loss of Sanicro 28 in Biomass boiler at 500 °C after 3000h

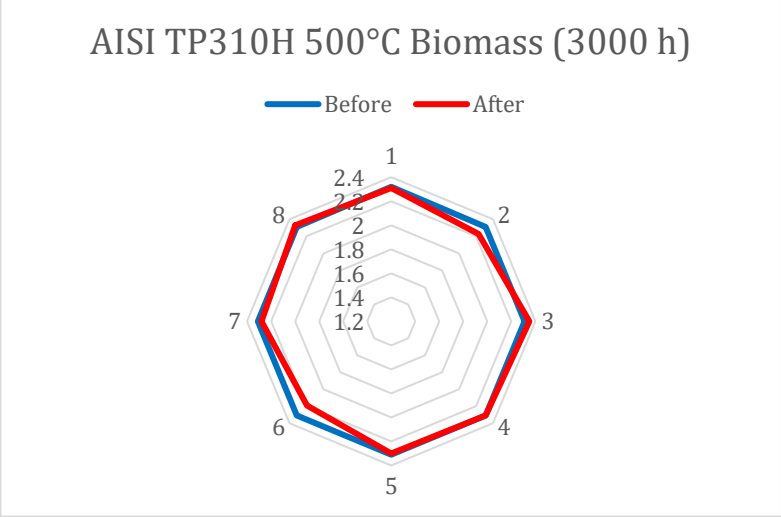

Figure 27, Material loss of AISI TP310H in Biomass boiler at 500 °C after 3000h

In figures 15-17 the material loos of the samples from 500 °C in the biomass boilers have been illustrated into graphs. The material with the greatest loss was P91 which was to be expected after looking at the SEM images of the three samples. The other two samples, being Sanicro 28 and AISI TP310H, have a relative low material loss with AISI TP310H having the lowest of the two. Below in table 4 the average and maximum material loss of each sample is presented.

Table 88. Average and maximum material loss of 500°C biomass samples

Samples 500 °C Biomass	**Average loss (mm)**	**Maximum Loss (mm)**	**Material loss after 8000h (average mm)**
P91	0.17	0.29	0.45
Sanicro 28	0.09	0.15	0.24
AISI TP310H	0.02	0.12	0.05

5.2.2 Waste boiler samples 500 °C

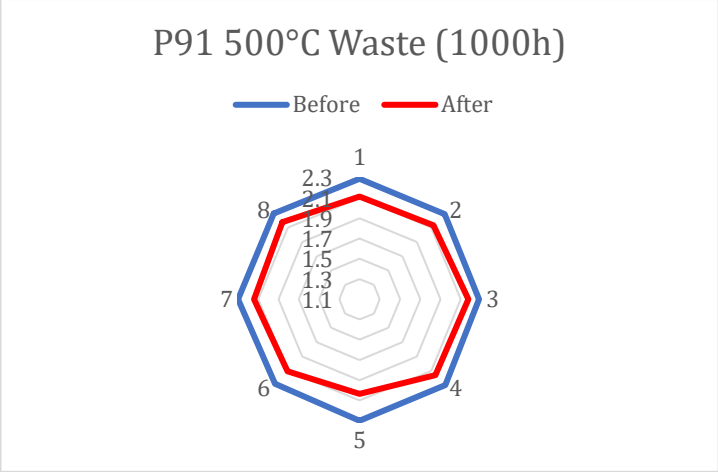

Figure 28. Material loss of P91 in Waste boiler after 1000h

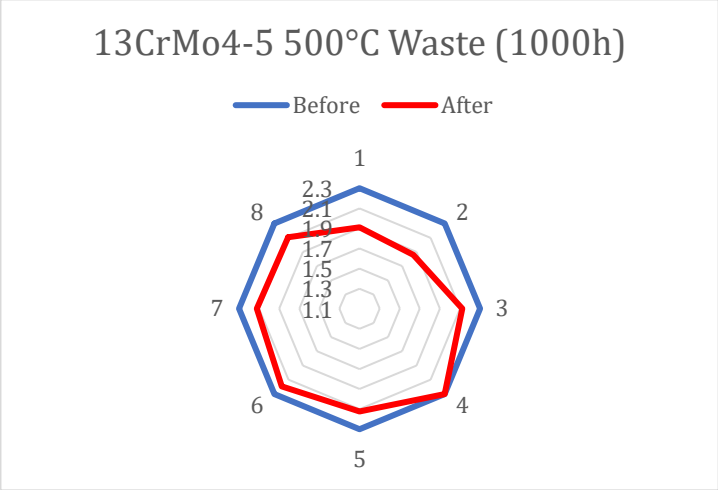

Figure 29. Material loss of 13CrMo4-5 in Waste boiler at 500°C after 1000h

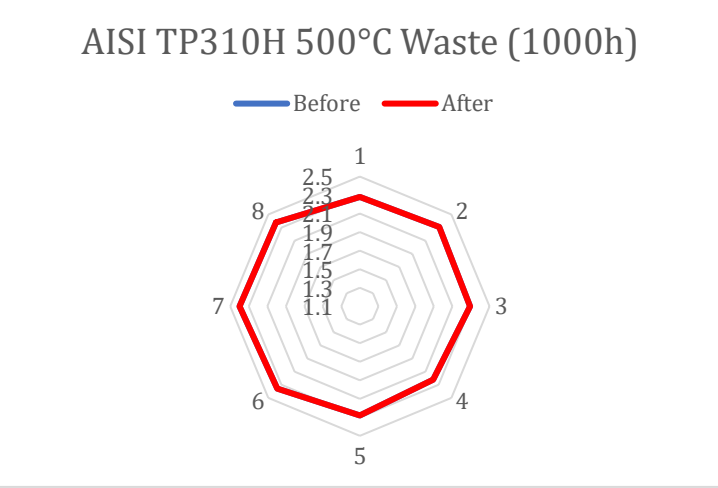

Figure 30. Material loss of AISI TP310H in Waste boiler at 500 °C after 1000h

In figures 18-20 the material loss of the samples in the waste boiler at 500 °C have been illustrated similarly to the ones from the biomass boiler at 500 °C. Of the samples in the waste boiler 13CrMo4-5 is the one with the highest material loss at 0,4 mm as its maximum. In the waste boiler the difference between the sample's material loss is greater than with the biomass samples as is shown in table 5 below.

Table 99. Average and maximum material loss of 500 °C waste samples

Samples 500 °C Waste	Average loss (mm)	Maximum loss (mm)	Material loss after 8000h (average mm)
P91	0.16	0.27	1.28
13CrMo4-5	0.24	0.44	1.92
AISI TP310H	0	0	0.08

5.2.3 Biomass boiler samples 600 °C

Table 1010. Average and maximum material loss of 600 °C biomass samples

Samples 600 °C B	Average loss (mm)	Maximum loss (mm)	Material loss after 8000h (average mm)
P91	n/a	n/a	n/a
Sanicro 28	n/a	n/a	n/a
AISI TP310H	n/a	n/a	n/a

The table above is based upon calculations and assumptions from SEM images. According to material loss data from samples exposed to 500 °C it would be appropriate to suppose that samples exposed to 600 °C for the same amount of time would show a greater material loss, or at least the same amount. For the three samples above together with the two samples from table 7, there is a general trend of a close to zero material loss calculated at the 8 spots around each sample. However, at many spots there is a "material growth" which is not possible. Therefore, an error has most likely occurred. One theory is that the scale in the images is wrong and therefore also the calculations. The samples are not totally flat after the cutting so the thickness measurement using SEM can be affected by the angle generated with the cut. The exact values of average loss, maximum loss and material loss after 8000 hours has therefore been left out of this study.

5.2.4 Waste boiler samples 600 °C

Table 1111. Average and maximum material loss of 600 °C waste samples

Samples 600 °C Waste	Average loss (mm)	Maximum loss (mm)	Material loss after 8000h (average mm)
Sanicro 28	n/a	n/a	n/a
AISI TP310H	n/a	n/a	n/a

The values in table 7 have been left out of this study. See section 5.2.3.

5.3 Ion Chromatography

The amount of SO_4 and Cl in each of the samples from the ion chromatography are presented below. The result is separated into two parts, the biomass samples and the waste samples.

In the result of the ion chromatography analysis, we can see that there is almost 0% Cl in the deposit from the four different samples. In the samples containing chlorine the amount can be

≈0 due to its low value. The extremely low amount of chlorine in the deposit of all the samples is good for the boilers as chlorine is much more corrosive than SO_4. Chlorine is more dangerous to metals then SO_4 for its ability to break apart the passive film of oxide at the edge of the metals. The destruction of passive film can cause pitting corrosion in the area in which the film has been removed.

5.3.1 Biomass boiler samples

The results from the IC of the Biomass samples at both 500°C and 600°C:

Table 1212. Biomass samples IC result

	SO_4 ppm	*Cl ppm*	*Mass of deposit*	*SO_4% Of deposit*	*Cl % of deposit*
500 °C Biomass	4387.9	0.4737	2.236	19.6	0.0212
600 °C Biomass	4555.8	n/a	2.885	15.8	n/a

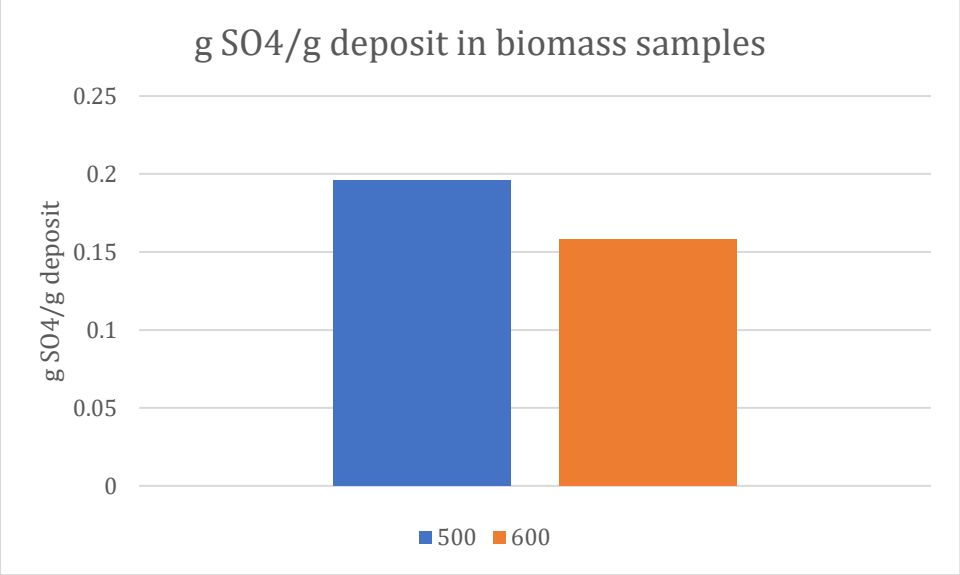

Figure 31. Difference in amount of SO4 in deposit of Biomass samples at 500 °C and 600 °C

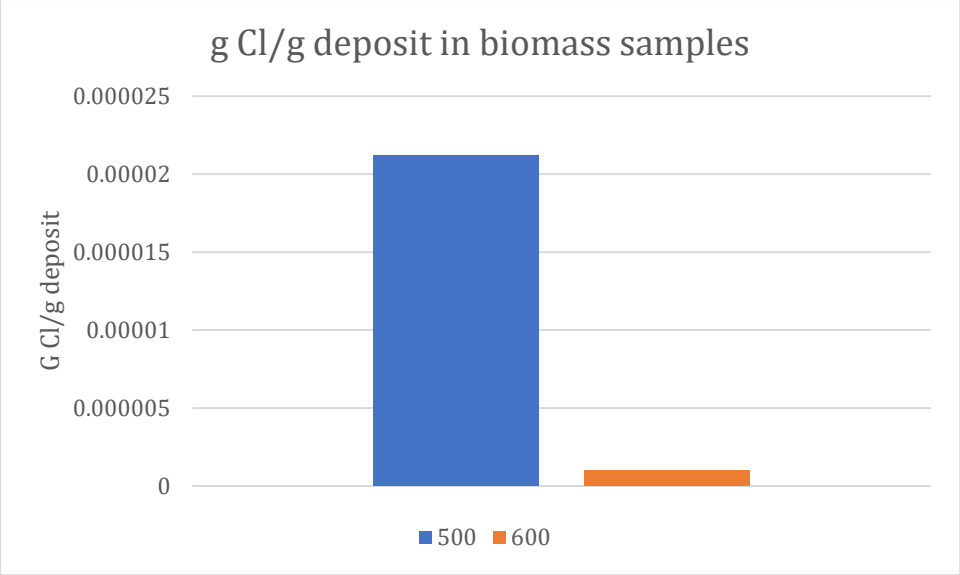

Figure 32. Difference in amount of Cl in deposit of Biomass samples at 500 °C and 600 °C

5.3.2 Waste boiler samples

The result from the IC of the Waste boiler samples at both 500°C ad 600°C:

Table 1313. Waste samples IC result

	SO_4 ppm	*Cl ppm*	*Mass of deposit*	*SO_4% Of deposit*	*Cl % of deposit*
500 °C Waste	5837.4	0.1413	6.09	9.45	0.0012
600 °C Waste	2203.8	n/a	3.52	6.26	n/a

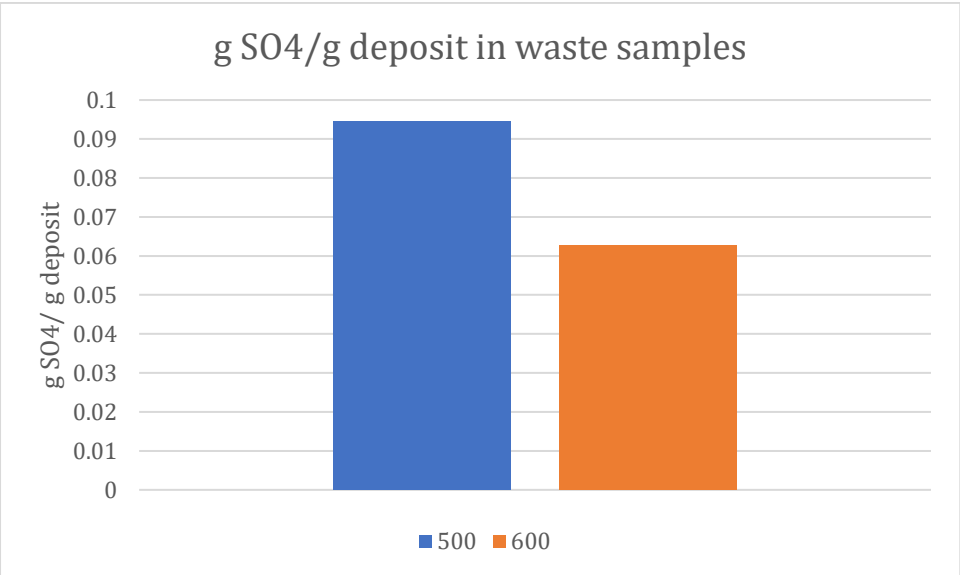

Figure 33. Difference in amount of SO4 in deposit of Waste samples at 500°C and 600°C

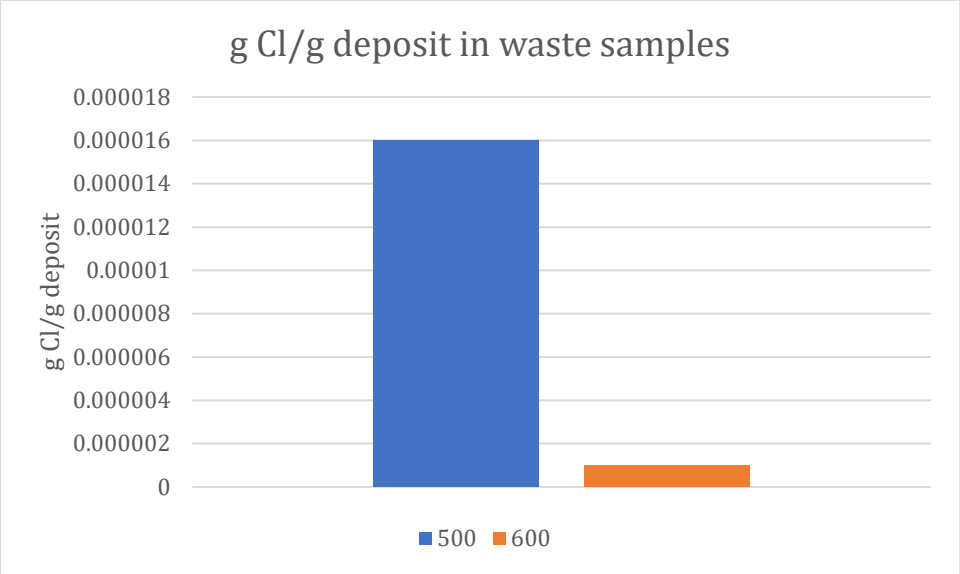

Figure 34. Difference in amount of Cl in deposit of Waste samples at 500°C and 600°C

6. Conclusions

So, which of the sample metals is best suited for the task of constructing boilers? In theory Sanicro 28 should be the metal with highest corrosion resistance due to the high amounts of nickel and chromium in the metal. However, when looking at the data from the study AISI TP310H samples have a lower material loss then the Sanicro 28 samples both after 3000h and 8000h. AISI TP310H gave the best protection of the three samples in the waste boiler after 1000h as could be seen in the SEM and EDX result. From a corrosion protection point of view AISI TP310H is the most suitable material for the boilers. There is however the economic aspect of the construction where the cheapest material is 13CrMo4-5 and the most expensive material is Sanicro 28. In this case, where AISI TP310H has proven to give the best protection against corrosion, and has moderate price when compared to Sanicro 28, it is the best option regarding the two major aspects when constructing a boiler.

7. Goal fulfilment and future research

This research has successfully gathered data regarding ten different steel alloys. Data that includes material loss and deposit layer analysis. Data that has been evaluated together with price comparisons to form a proposition of which steel alloy that is best suitable for the boilers. One incomplete part of the study is the samples exposed to 600 °C. Data was acquired but results did not match expectations and unfeasible values where calculated. Therefore, future research is needed to determine the effect of 600 °C exposure.

8. Literature references

[1] D. Jones, Global Electricity Review 2022 (2022, 30, mars), EMBER Available at: https://ember-climate.org/insights/research/global-electricity-review-2022/

[2] H. Ritchie, M. Roser, Electricity Mix (2022), Our World in Data, Available at: https://ourworldindata.org/electricity-mix

[3] T.R. Miles, T.R. Miles Jr., L.L. Baxter, R.W. Bryers, B.M. Jenkins, L.L. Oden, Boiler deposits fromfiring biomass fuels, Biomass Bioenergy 10 (1996) 125–138

[4] L. Paz, A. Olivas, T. Jonsson, A. Pettersson, F. Moradian, A. Jonasson, J. Aspen, P. Schneider, J. Mahanen, K. Vvänskä, V. Barisic, B. Jönsson, J. Hernblom, M. Huhtakangas, J. Liske, Combating high temperature corrosion by new materials, testing procedures and improved chemical selection, Energiforskning (2018)

[5] J. Pettersson, N. Folkeson, J.-E. Svensson, L.-G. Johansson, The effects of KCl, K2SO4and K2CO3on the high temperature corrosion of a 304-type austenitic stainlesssteel, Oxid. Met. 76 (2011) 93–109.

[6] Which Metals/Alloys are Oxidation Resistant? (super-metals.com)

[7]Corrosionpedia, Passive film (2019,12,september), Available at: https://www.corrosionpedia.com/definition/1615/passive-film

[8] Longhaisteel, 13CrMo4-5 (2015), Available at: 13CrMo4-5Chemical composition,properties,Datasheet (steelss.com)

[9] A. Norlander, 13CrMo4-5 (2023), Livallco stål AB, Available at: Stål material 13crmo4-5 | 1.7335 ▷ SS 2216 | Livallco®

9. Appendices

Mat loss images for Biganos (500° C)


P91.pdf


Sanicro 28.pdf


TP310H.pdf

Mat loss images for Biganos (600° C)


P91.pdf


Sanicro 28.pdf


TP310H.pdf

Mat loss images for Grenoble (500° C)


P91.pdf


13CrMo4-5.pdf


TP310H.pdf

Mat loss images for Grenoble (600° C)


Sanicro 28.pdf


TP310H.pdf

Extra SEM images Biganos


TP310H - 500°C.pdf


TP310H - 600°C.pdf


P91 - 500°C.pdf


P91 - 600°C.pdf


Sanicro 28 - 500°C.pdf


Sanicro 28 - 600°C.pdf

Extra SEM images Grenoble


13CrMo4-5 - 500°C.pdf

TP310H - 500°C.pdf

TP310H - 600°C.pdf

P91 - 500°C.pdf

Sanicro 28 - 600°C.pdf

DEPARTMENT OF CHEMISTRY AND
CHEMICAL ENGINEERING
CHALMERS UNIVERSITY OF TECHNOLOGY
Gothenburg, Sweden 2023
www.chalmers.se

CHALMERS